Ain Shams Engineering Journal xxx (xxxx) xxx

Contents lists available at ScienceDirect

Ain Shams Engineering Journal

journal homepage: www.sciencedirect.com

Electrical Engineering

Economical-technical-environmental operation of power networks with wind-solar-hydropower generation using analytic hierarchy process and improved grey wolf algorithm

Muhyaddin Rawa [a,b], Abdullah Abusorrah [a,b], Hussain Bassi [a,c], Saad Mekhilef [a,d], Ziad M. Ali [e,f,*], Shady H.E. Abdel Aleem [g,h], Hany M. Hasanien [i], Ahmed I. Omar [j]

[a] Center of Research Excellence in Renewable Energy and Power Systems, King Abdulaziz University, Jeddah 21589, Saudi Arabia
[b] Department of Electrical and Computer Engineering, Faculty of Engineering, King Abdulaziz University, Jeddah 21589, Saudi Arabia
[c] Department of Electrical Engineering, Faculty of Engineering, King Abdulaziz University, Rabigh 25732, Saudi Arabia
[d] Power Electronics and Renewable Energy Research Laboratory, Department of Electrical Engineering, University of Malaya, 50603 Kuala Lumpur, Malaysia
[e] Electrical Engineering Department, College of Engineering at Wadi Addawaser, Prince Sattam Bin Abdulaziz University, 11991, Saudi Arabia
[f] Electrical Engineering Department, Aswan Faculty of Engineering, Aswan University, 81542, Egypt
[g] Technology and Maritime Transport, Electrical Energy Department, The College of Engineering and Technology, Arab Academy for Science, Giza 12577, Egypt
[h] Power Quality Solutions, ETA Electric Company, El Omraniya, Giza 12111, Egypt
[i] Faculty of Engineering and Technology, Future University in Egypt, Cairo 11835, Egypt
[j] Electrical Power and Machines Engineering, The Higher Institute of Engineering at El-Shorouk City, Egypt

ARTICLE INFO

Article history:
Received 29 December 2020
Revised 16 January 2021
Accepted 10 February 2021
Available online xxxx

Keywords:
Analytic hierarchy process
Energy
Economical-technical-environmental dispatch
Improved grey wolf algorithm
Optimal power flow
Power systems
Renewable energy sources

ABSTRACT

This paper presents an economical-technical-environmental dispatch (ETED) model for an adapted IEEE 30-bus system incorporated with thermal and a mix of renewable energy sources (RESs). Total fuel costs, active power losses, and emissions level minimization is the main aim. Different equality and inequality limits involving prohibited operating zones (POZs) are considered as system restrictions. Metaheuristic optimization techniques – moth-flame optimization, salp swarm algorithm, improved grey wolf optimizer, and multi-verse optimizer – are employed to find the best solution for the generation cost, losses, and emissions. Various scenarios are examined to approve the ability of the formulated optimization model in solving the problem. A weighted sum strategy using the analytic hierarchy process (AHP) is used to convert the multi-objective problem into a normalized single-objective one. The AHP-ETED model presented in this work can significantly minimize fuel costs to 902.4951 $/h, lower emission levels as 0.09785 t/h, and achieve a lower power loss of 2.4110 MW. The results attained validate that the IGWO outperforms the other considered algorithms in finding the best solution to the ETED problem.

1. Introduction

The stochastic nature of renewable energy sources (RESs) has formed a challenge to incorporate them into the traditional power grids. The expansion in RESs units' use has revealed the techno-economic problems of traditional thermal generation plants [1]. In order to face the uncertainty challenges in renewable generation planning and help support smooth renewable penetration into power grids, it is of great importance to involve the stochastic nature of photovoltaic, wind, and hydropower plants [2]. Concerning these challenges, it is crucial that the power grid is operating economically with a high degree of reliability in order to provide the stakeholders in the related power market with a fair, competitive situation [3]. Environmentally speaking, thermal power plants

* Corresponding author at: Electrical Engineering Department, College of Engineering at Wadi Addawaser, Prince Sattam Bin Abdulaziz University, 11991, Saudi Arabia.
E-mail addresses: mrawa@kau.edu.sa (M. Rawa), aabusorrah@kau.edu.sa (A. Abusorrah), hmbassi@kau.edu.sa (H. Bassi), saad@um.edu.my (S. Mekhilef), z.ali@psau.edu.sa, dr.ziad.elhalwany@aswu.edu.eg (Z.M. Ali), engyshady@ieee.org (S.H.E. Abdel Aleem), hanyhasanien@ieee.org (H.M. Hasanien), a.omar@sha.edu.eg (A.I. Omar).

Peer review under responsibility of Ain Shams University.

Production and hosting by Elsevier

https://doi.org/10.1016/j.asej.2021.02.004
2090-4479/

produce multi-pollutant gas emissions as nitrogen oxide, carbon oxides (carbon monoxide and carbon dioxide), sulfur dioxide, and others [4]. The reliance on renewables reduces the need for fossil fuels, thus reducing the associated emission levels of the traditional plants using these fuels. Furthermore, the power system operation can be enhanced by lowering network power losses, increasing energy efficiency, supporting voltage, and deferring investments to upgrade power systems. This problem can be solved by formulating an economical-technical-environmental dispatch (ETED) model. The prime goal line of the ETED is to decrease the fuel cost of generating units, reduce power losses in power grids, and minimize the emission levels of the thermal units in order to optimize the system performance and reduce costs [5].

A variety of conventional approaches used in solving optimization problems (OPs), such as based-point and participation coefficients, linear and quadratic iterative methods [6], lambda iteration-based methods [7], and gradient approaches [8], were presented in the literature for solving the traditional economical-environmental dispatch (EED) problem. Due to the EED problem's complexity, most of these approaches have faced difficulties finding global solutions at an appropriate computation time [9]. Consequently, researchers sought to apply the updated formulations of powerful mathematical-based optimization techniques to solve the EED problem like mixed-integer programming, linear type (MILP) and quadratic type (MIQP), non-linear programming (NLP), and dynamic programming (DP) [10,11]. For instance, in [12], the NLP approach (a fractional type of Dinkelbach's algorithm) was used to solve the problem, in which that approach aimed to minimize the generation cost and pollutant emissions formed from the use of traditional generators. However, different operational constraints were not addressed in this work. Pan et al. [13] presented a combination between MILP and the interior point approach (IPA) to solve the same problem while considering the transmission line losses and valve points. However, that approach did not have prohibited operational zones (POZs) restrictions. It was mentioned that difficulty is noticed in calculating transmission losses precisely because of numerous generating units. Most of the conventional mathematical-based optimization approaches face significant difficulties in coping with large-scale generation-mixed power systems. They are often getting tapped into local minima because of the tendency to oscillate their decision parameters during the optimization runs, and this significantly increases the calculation time.

Recently, numerous metaheuristic optimization techniques for single-objective (SO) and multi-objective (MO) functions have been introduced in the literature with and without the incorporation of RESs to overcome the previously-mentioned shortcomings [14,15]. Various evolutionary and metaheuristic optimization techniques were efficiently employed to solve the optimal power flow problem, like improved MO moth-flame optimization (IMOFO) [16], enhanced whale optimization algorithm (EWOA) [17], particle swarm optimization (PSO) with time-varying acceleration coefficient, so-called TVAC-PSO [18], accelerated PSO (APSO) [19], the interior search algorithm (ISA) [20], a combination of PSO and salp swarm algorithm (SSA) [21], dynamic population-based artificial bee colony (ABC), so-called ABC-DP [22], ABC [23], MO cross-entropy algorithm based on decomposition (MOCE/D) [24], MO population extremal optimization (MOPEO) [25], summation-based MO differential evolution (SMODE) [26], and a MO algorithm based on decomposition (MOEA/D) [27]. Some took into account the presence of RESs, and some did not take them into account when solving their optimization issue. For instance, Wang et al. [24] proposed the MOCE/D to solve the problem while considering a hybrid wind- hydropower-photovoltaic plants in the model, while complying with the operational limitations, POZs restrictions, and the RESs' intermittences. The impact of valve points on the system performance was not involved. Chen et al. [25] used the MOPEO approach to reduce costs and emissions in a modified IEEE 30-bus system with RESs. In [28], a non-dominant sorting genetic algorithm (NSGA-II) integrated with a reinforcement learning approach, named NSGA-RL, was employed by Bora et al. to reduce fuel costs emissions of six thermal generators and added wind turbines. The obtained results solved the EED problem with the NSGA-RL method. Likewise, in [26], MOEA/D and SMODE were efficiently used for costs and emissions minimization in the 30-bus system, with limited thermal plants and stochastic RESs. Yin et al. [29] proposed a complex day-ahead scheme with mixed stochastic RESs in the model to minimize the fuel costs. In [30], the authors introduced a MOMFO strategy to solve the complex EED with hybrid RESs based on tradeable green certificates without considering the power flow's nonlinear limits in the problem. In [31], the improved shuffled frog leaping algorithm (ISFLA) for solving the EED problem was used in the optimal power flow problem formulation with combined heat and power (CHP) for lowering fuel costs and emissions. One can see that the multiple works in this area have demonstrated the importance of solving this issue in modern power systems with renewables [32,33].

However, many articles have been interested in showing modern optimization algorithms at the expense of the presence of RESs in their systems. For instance, Medani et al. [17] suggested EWOA for real power loss minimization, but no RESs were included in this approach. The results verified that EWOA was stable and effective in achieving the optimum solution and quickly reducing power loss. Modiri et al. [34] used a backtracking search algorithm (BSA) to solve the EED of fuel costs and emissions problems. Diverse optimization algorithms have been introduced to analyze the performance of the systems being studied, but the effect of valve points and POZs was not considered when presented. Also, Mason et al. [19] addressed PSO variants in which two objective functions of costs and emission levels have been modeled while taking into account the hourly power demand intermittency. The obtained results have been compared to other optimization algorithms to demonstrate PSO variants' efficiency. In [18], the authors suggested using TVAC-PSO to solve the EED problem with 48 CHP units as a case study. The results obtained revealed the methodology's ability to solve the problem. The IMFO algorithm was used by Elsakaan et al. in [16]. However, different limitations, like POZs and system security, were not considered in the methodology used. In [21], the authors have proposed a combined SSA and PSO optimization method in solving the EED problem. The method presented has been applied to solve SO and MO strategies with multiple objectives, like minimizing the cost of generation, pollution, power loss, and enhancing the system voltage's stability. In [27], the authors introduced the MOEA/D technique in the IEEE 30- and 57-bus systems to solve the EED with a small number of limitations to minimize the emission, cost, and power loss and deviations of voltage. Yet, no method has been proved to be the best optimizer in solving the EED problem with renewables to date. The usual main objective of energy utilities is to meet consumer requirements but to lessen the cost of fuel and decrease power losses without taking into account pollutant emissions [35]. But it is worth noting that the various countries have begun today to help protect the atmosphere from carbon emissions using many new methods and approaches for reducing pollutants to meet national and international environmental protection requirements; otherwise, they would be globally penalized. The reduction of fuel costs of production units in electrical networks also plays an essential role in fulfilling the loads' demands in the ETED problem. Diminishing carbon emissions is seen as one of the most critical factors for overcoming climate change and environmental degradation. The objective function is interpreted and formulated as a SO-OP in the simple ETED formulation. However, to lower greenhouse

gas emissions, the ETED problem is tackled by matching different targets simultaneously. The optimal key is incorporating RESs in electrical networks to reduce such pollution while cost-effectively achieving the technical merits.

In this article, the IEEE 30-bus scheme is amended to incorporate photovoltaic (PV) units, a wind generator (WG), and a hydropower (HP) plant with a restricted number of thermal generators. The uncertainties of PVs, HP, and WGs are analyzed in detail, using appropriate probability density functions (PDFs) – lognormal, Gumbel, and Weibull, respectively [36]. Both underestimation penalty cost (UPC) and overestimation reserve cost (ORC) are included in the cost model presented in this work to handle the uncertainty and intermittency of the RESs. Moth-flame optimization (MFO), salp swarm algorithm (SSA), improved grey wolf optimizer (IGWO), and multi-verse optimizer (MVO) are employed as SO optimization techniques to find the generation cost, losses, and emissions. Different scenarios are investigated to evidence the proposed mode's ability to solve the problem. After that, a weighted sum strategy using the analytic hierarchy process (AHP) is employed to convert the MO-ETED problem into a normalized SO-ETED one.

The rest of the paper is structured as follows. The system's formation is presented in Section 2. The mathematical formulation of the ETED problem integrating RESs, formulation of the objective functions, and design of linear and non-linear constraints are presented in Section 3. The proposed optimization methods are presented in Section 4. Results got are explored and discussed in Section 5. Finally, conclusions and future works are given in Section 6.

2. The system under study

The IEEE 30-bus adoption is addressed in this work, which involves both conventional thermal generators and modern RESs [37]. As illustrated in Fig. 1, three separate RESs of wind, PV, and hybrid PV and hydropower (PVHP) systems are connected to buses 5, 11, and 13, respectively. This model also includes three thermal generators (TGs) connected to buses 1, 2, and 8 [2]. The essential system's parameters are given in Table 1.

First, individual scenarios are examined to understand the minimization of the fuel costs-power losses-emissions alone. In the scenarios, we commonly have utilized three RESs – WG (bus 5), PV (bus 11), and PVHP plant (bus 13). They have formulated as a SO-OP: Scenario I using the fuel costs as the objective function, Scenario II using the power losses, and Scenario III using the emission levels as the objective function. Second, the weighted sum approach, one of the most widely used methods due to its simplicity, was used to convert the MO problem into a scalar normalized one by constructing a weighted sum of all the objectives.

In this regard, an important issue is choosing the weighting coefficients; hence, an equal weighting coefficients scenario (denoted as Scenario IV) was applied to have a general picture of the preference function's performance. Further, a weighted sum strategy using AHP (designated as Scenario V) was used to assign a preference order to the MOs with weights that reflect the preference of the decision-maker.

Besides, four optimization approaches – SSA, MFO, MVO, and IGWO are implemented to solve the problem under study. The procedure of the scenarios and the optimization methods is illustrated in Fig. 2.

3. Formulation of the objective function

The ETED problem is carried on by simultaneously minimizing three computing fitness functions – fuel cost, losses, and emissions, with different equality and inequality restrictions. Generally, the ETED problem is interpreted and framed as follows:

$$\text{Minimize}(ETED) = \min(J_1, J_2, J_3) \tag{1}$$

where, J_1, J_2, and J_3 represent the objective functions of total fuel costs, power losses, and emissions to be minimized, respectively.

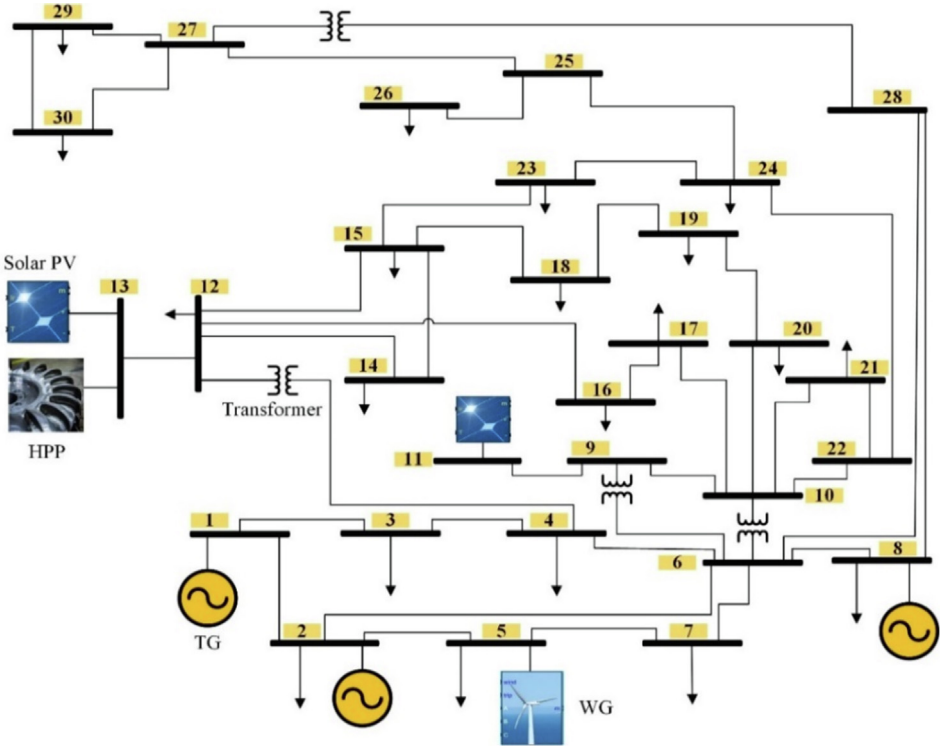

Fig. 1. The system under study.

Table 1
Parameters of the system [27].

Elements	Quantity	Parameters
Generators	6	3 TGs and 3 RESs
TGs	3	Buses 1*, 2, and 8
WG	25	Bus 5, 75 MW
PV	1	Bus 11, 50 MW
PVHP	1	Bus 13, 45 + 5 MW
Load demand (P and Q)	–	283.40 MW and 126.20 MVAr
Number of PQ buses	24	24 buses
Permissible load voltage range (pu)	–	0.95–1.10

* Bus 1 is the slack bus.

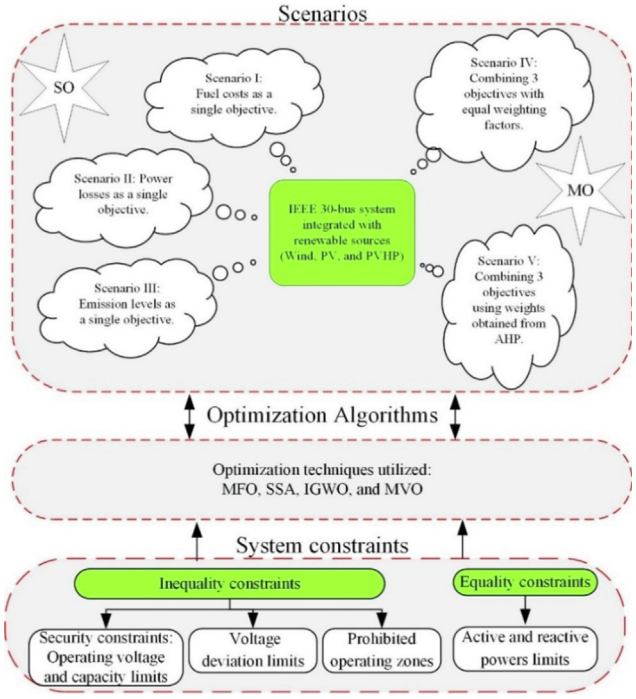

Fig. 2. The procedure of the presented methods.

The triple-objective ETED problematic model is transformed into the simple SO-OP by introducing weighting factors as follows:

$$\text{Minimize}(ETED) = \min\left(w_1 \times \left|\frac{F_{tot}}{J_1}\right| + w_2 \times \left|\frac{P_{Losstot}}{J_2}\right| + w_3 \times \left|\frac{E_{tot}}{J_3}\right|\right) \quad (2)$$

where, w_1, w_2, and w_3 represent the weighting factors of the total fuel costs (F_{tot}), power losses ($P_{Losstot}$) and emissions (E_{tot}), respectively.

3.1. Objective 1

The summation of costs of the TGs and RESs expresses the total cost, as given in (3).

$$\text{Min}(J_1) = \min(F_{tot}) = F_{tot}(P_{TGs}) + F_{tot}(P_{RESs}) \quad (3)$$

where, $F_{tot}(P_{TGs})$ and $F_{tot}(P_{RESs})$ denote the total TGs cost and the total RESs cost, respectively.

TGs's fuel cost: The TGs cost, in $/MWh, mainly depends on the steam flow to the blades and the unexpected changes in the position of the valves. A set of valves drives steam in these plants for turbine operation via a dispersed group of nozzles used at full production to get good performance [38]. These valves are opened in sequence for the obligatory operation, which causes a cut-out in the cost curve (discontinuous cost curve), as shown in Fig. 3. $F_{tot}(P_{TGs})$ is expressed in (4) [39], thus:

$$F_{tot}(P_{TG}) = \sum_{i=1}^{N_{TG}} a_{TG_i} + b_{TG_i}P_{TG_i} + c_{TG_i}P_{TG_i}^2 + \left|d_i \times \sin\left(e_i \times \left(P_{TG_i}^{min} - P_{TG_i}\right)\right)\right| \quad (4)$$

where $a_{T_{Gi}}$, b_{TG_i} and c_{TG_i} denote the cost factors of the ith TGs (P_{TG_i}). d_i and e_i denote the effect of valve point.$P_{TG_i}^{min}$ denotes the minimum power of P_{TG_i} throughout the operation.

RESs' cost: The RESs cost ($/MWh) is the summation of the total costs of PVs ($F_{tot}(P_{PV})$), WGs ($F_{tot}(P_{WG})$) and PVHP ($F_{tot}(P_{PVHP})$) as expressed in (5).

$$F_{tot}(P_{VRES}) = F_{tot}(P_{PV}) + F_{tot}(P_{WG}) + F_{tot}(P_{PVHP}) \quad (5)$$

Each RES has a definite function to express its cost. The amount of under-or over-delivered power can be estimated using the RES's PDF.

To handle the intermittence nature of these RESs, standby generators (SGs) could be connected whenever the scheduled power exceeds the produced one. Storage batteries can be connected to reserve the additional energy produced [40].

Cost estimation of WGs ($C_{tot_{WG}}$): $C_{tot_{WG}}$ is expressed by combining the direct investment costs ($C_{d_{WG}}(P_{WGsch})$) in addition to the SGs and storage units costs. $C_{d_{WG}}(P_{WGsch})$ represents the initial, operational, and maintenance costs as given in (6).

$$C_{d_{WG}}(P_{WGsch}) = K_{d_{WG}} \times P_{WGsch} \quad (6)$$

where $K_{d_{WG}}$ denotes the direct cost factor and P_{WGsch} represents the WGs' scheduled power. The system also may include likely standby units to preserve the demand needs (i.e., reserve capacity potential to safeguard the needs of the demand), and this reserve cost capacity cost ($C_{r_{WG}}$) is formulated as follows:

$$C_{r_{WG}}(P_{WGsch} - P_{WG_{act}}) = K_{r_{WG}}(P_{WGsch} - P_{WG_{act}}) = K_{r_{WG}} \times \int_0^{P_{WG_{act}}} (P_{WGsch} - p_{wT}) f_{wT}(p_{WG}) dp_{wT} \quad (7)$$

$K_{r_{WG}}$ denotes the cost factor of the standby units and $P_{WG_{act}}$ denotes the actual WGs' delivered power. Likewise, If $P_{WGsch} < P_{WG_{act}}$; then the storage units cost, expressed in (8), will be added to the total WG cost. The cost coefficients of WGs are presented in Appendix A.

$$C_{s_{WG}}(P_{WG_{act}} - P_{WGsch}) = K_{s_{WG}}(P_{WG_{act}} - P_{WGsch}) = K_{s_{WG}} \int_{P_{WGsch}}^{P_{WGr}} (p_{WG} - P_{WGsch}) f_w(p_{WG}) dp_{wT} \quad (8)$$

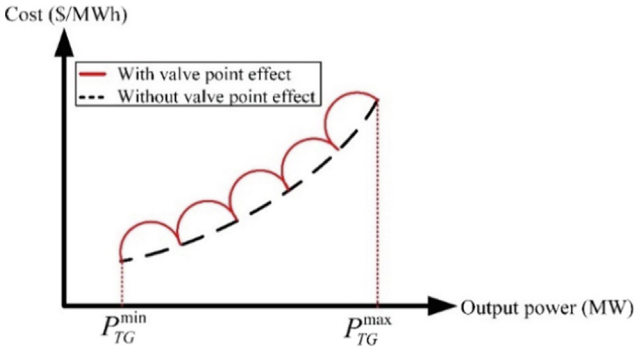

Fig. 3. Discontinuous cost curve because of the operation of the point valves.

where P_{WGr} ,$f_w(p_{wT})$ denote the rated wind power and the wind speed (v)'s PDF, respectively. The storage units and standby powers rely on $f_w(p_{wT})$. Weibull distribution (WD) is commonly used to fit the random frequency of each v measure [41,42]. Fig. 4(a) shows the WD-based PDF of v data spreading over 8000 Monte-Carlo runs. The scale (α) and the shape (β) coefficients of the WD-based PDF are considered as 9 and 2, respectively. The probability ($f_v(v)$)of v is shown in (9):

$$f_v(v) = \left(\frac{\beta}{\alpha}\right)\left(\frac{v}{\alpha}\right)^{(\beta-1)} e^{-(v/\alpha)^{\beta}} \text{for} 0 < v < \infty \tag{9}$$

The WGs' provided power that relies on v is expressed by (10):

$$p_{wT} = \begin{cases} 0 v_{out} \le v \le v_{in} \\ P_{WGr}\left(\frac{v - v_{in}}{v_r - v_{in}}\right) v_{in} \le v \le v_r \\ P_{WGr} v_r \le v \le v_{out} \end{cases} \tag{10}$$

where, v_{in}, v_{out}, v_r represent the WGs' cut-in, cut-out, and rated speeds, respectively. The probability of wind power $f_w(p_{wG})$ is given in (11).

$$f_w(p_{wG}) = \frac{\beta(v_r - v_{in})}{\alpha^{\beta} \times P_{Wr}}\left[v_{in} + \frac{p_{wG}}{P_{WGr}}(v_r - v_{in})\right]^{\beta-1} \times \exp\left[-\left(\frac{v_{in} + \frac{p_{WG}}{P_{WGr}}(v_r - v_{in})}{\alpha}\right)^{\beta}\right] \tag{11}$$

To sum up, $C_{tot_{WG}}$ is expressed in (12).

$$C_{tot_{WG}} = C_{d_{WG}}(P_{WGsch}) + C_{r_{WG}}(P_{WGsch} - P_{WG_{act}}) + C_{s_{WG}}(P_{WG_{act}} - P_{WGsch}) \tag{12}$$

Cost estimation of the PV ($\boldsymbol{C_{tot_{PV}}}$): Likewise, the solar plant's total cost function has been constructed based on the same attitude utilized to estimate the WGs' cost function. The direct cost $\boldsymbol{C_{d_{PV}}(P_{PVsch})}$ of PVs denotes the initial, operational, and maintenance costs, and is given in (13).

$$C_{d_{PV}}(P_{PVsch}) = K_{d_{PV}} \times P_{PVsch} \tag{13}$$

where $K_{d_{PV}}$ denotes the direct cost coefficient and P_{PVsch} denotes the scheduled PV system power.

When $P_{PVsch}$is greater than the PV system's actual power (P_{PVact}), it is essential to carry out SGs, as explained earlier. The PV's reserve capacity ($C_{r_{PV}}$) cost is given in (14).

$$C_{r_{PV}}(P_{PVsch} - P_{PV_{act}}) = K_{r_{PV}}(P_{PVsch} - P_{PV_{act}}) = K_{r_{PV}}(P_{PVsch} - p_{PV}) \times f_{PV}(p_{PV}) \tag{14}$$

$K_{r_{PV}}$ denotes the cost parameter of the SGs. Also, the storage units ($C_{s_{PV}}$) cost may appear if $P_{PVsch} < P_{PV_{act}}$, and this is expressed in (15).

$$C_{s_{PV}}(P_{PV_{act}} - P_{PVsch}) = K_{s_{PV}}(P_{PV_{act}} - P_{PVsch}) = K_{s_{PV}}(p_{PV} - P_{PVsch}) \times f_{PV}(p_{PV}) \tag{15}$$

The cost coefficients of PV units are also presented in Appendix A. The delivered power from the standby and storage units relies on the solar irradiance (G) PDF, denoted as $f_{PV}(G)$. Lognormal distribution (LD) [43,44] is commonly used to get $f_{PV}(G)$, as shown in Fig. 4(b) for 8000 Monte-Carlo runs at lognormal fit factors: $\mu = 5.6$ and $\sigma = 0.6$. Hence, $f_{PV}(G)$ is given as:

$$f_{PV}(G) = \frac{1}{G\sigma\sqrt{2\pi}} \exp\left\{\frac{-(lnG - \mu^2)}{2\sigma^2}\right\}, \forall G > 0 \tag{16}$$

The obtainable PV's power can be estimated as given in (17):

$$p_{PV}(G) = \begin{cases} P_{PVr}\left(\frac{G^2}{G_{std}}\right), 0 < G < R_c \\ P_{PVr}\left(\frac{G}{G_{std}}\right), G \ge R_c \end{cases} \tag{17}$$

where G_{std} denotes the standard solar irradiance and R_c denote the operation irradiance, in which $G_{std} = 1000$ W/m^2, and $R_c = 120$ W/m^2. P_{PVr} denotes the PV units' rated output power. To sum up, $C_{tot_{PV}}$ is expressed in (18).

$$C_{tot_{PV}} = C_{d_{PV}}(P_{PVsch}) + C_{s_{PV}}(P_{PV_{act}} - P_{PVsch}) + C_{r_{PV}}(P_{PVsch} - P_{PV_{act}}) \tag{18}$$

Cost estimation of the PVHP plant ($\boldsymbol{C_{tot_{PVHP}}}$): Gumbel distribution (GD) [45] is used in the fitting of the river flow ($\boldsymbol{Q_w}$) data, as shown in Fig. 4(c), in which $\boldsymbol{f_Q(Q_w)}$ tracks the GD with parameters λ and γ as follows:

$$f_Q(Q_w) = \frac{1}{\gamma} exp\left(\frac{Q_w - \lambda}{\gamma}\right) exp\left[-exp\left(\frac{Q_w - \lambda}{\gamma}\right)\right] \tag{19}$$

The yield power from the hydropower plant $P_H(Q_w)$ mainly relies on Q_w as expressed in (20):

$$P_H(Q_w) = \eta_w \rho_w g_w Q_w H_w \tag{20}$$

where η_w, g_w, ρ_w,and H_w denote the hydro turbine's efficiency, the acceleration due to gravity, the density of water, and the effective pressure head, respectively [46], in which $\eta_W = 0.86$; $\rho_W = 1000$kg/m^3; $g_W = 9.81$m/s^2; and $H_w = 26$m. At this bus, the HP plant is integrated with a PV plant to improve the HP plant performance. To sum up, $C_{tot_{PVHP}}$ is expressed in (21).

$$C_{tot_{PVHP}} = C_{dPVHP}(P_{PVHPsch}) + C_{r_{PVHP}}(P_{PVHPsch} - P_{PVHP_{act}}) + C_{s_{PVHP}}(P_{PVHP_{act}} - P_{PVHPsch}) \tag{21}$$

where $P_{PVHPsch}$ and $P_{PVHP_{act}}$ denote the hybrid PVHP's scheduled and actual powers, respectively. $C_{dPVSH}(P_{PVHP})$ denotes the direct cost of the PVHP. $C_{r_{PVHP}}$ and $C_{s_{PVHP}}$ denote the SG and storage units costs, respectively. The cost coefficients of PVHP are presented in Appendix A.

Further, to compile all the cost functions, F_{tot} of the overall system is expressed as given in (22).

$$\begin{aligned} F_{tot} = & \sum_{i=1}^{N_{TPGU}} a_{TG_i} + b_{TG_i} P_{TG_i} + c_{TG_i} P_{TG_i}^2 \\ & + \left| d_i \times \sin\left(e_i \times \left(P_{TG_i}^{min} - P_{TG_i}\right)\right)\right| + C_{d_{WG}}(P_{WGsch}) \\ & + C_{r_{WG}}(P_{WGsch} - P_{WG_{act}}) + C_{s_{WG}}(P_{WG_{act}} - P_{WGsch}) \\ & + C_{d_{PV}}(P_{PVsch}) + C_{r_{PV}}(P_{PVsch} - P_{PV_{act}}) \\ & + C_{s_{PV}}(P_{PV_{act}} - P_{PVsch}) + C_{dPVHP}(P_{PVHPsch}) \\ & + C_{r_{PVHP}}(P_{PVHPsch} - P_{PVHP_{act}}) + C_{s_{PVHP}}(P_{PVHP_{act}} - P_{PVHPsch}) \end{aligned} \tag{22}$$

3.2. Objective 2

The active power loss (P_{loss}) of the electric network can be expressed as given in (23):

$$\text{Min}(J_2) = \min(P_{loss}) = \sum_{x=1}^{nl} G_{x(ij)}\left[V_i^2 + V_j^2 - 2V_iV_j\cos(\delta_{ij})\right] \tag{23}$$

where V_i and V_j represent the voltages at buses i and j, respectively. $\delta_{ij} = \delta_i - \delta_j$ denotes the voltage angle difference between buses i and j.

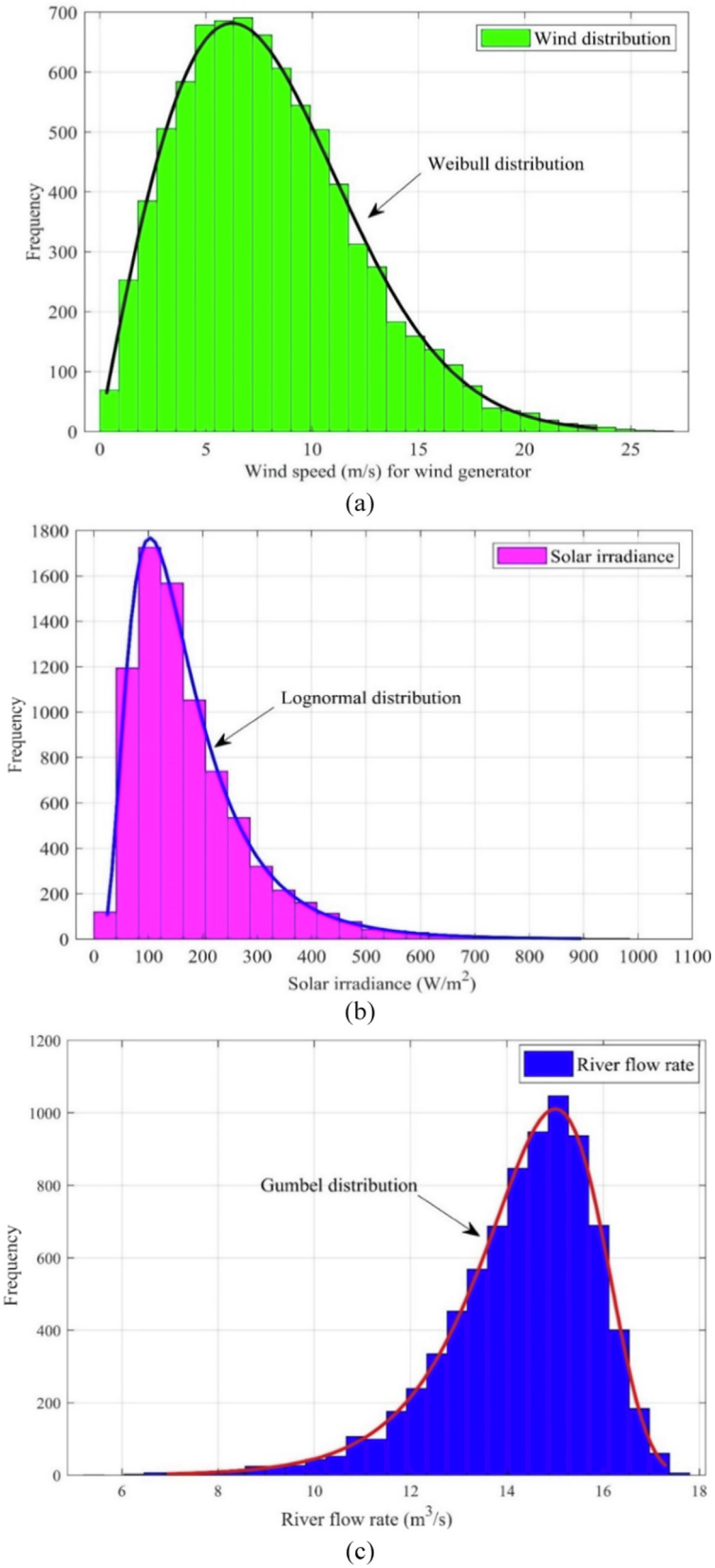

Fig. 4. Considered PDFs of wind speed, solar irradiance, and river flow rate: (a) WD, (b) LD, and (c) GD.

3.3. Objective 3

Only the emissions of TGs (E_{tot}) are considered because the RESs have few to no emissions, as given in (24):

$$\text{Min}(J_3) = \min(E_{tot}) = \sum_{i=1}^{N_{TG}} E_{TGi} \tag{24}$$

where E_{TGi} denotes the total emissions of the ith TG. The total emissions $E_{tot}(TG)$ is the sum of harmful gas emissions that negatively affects the atmosphere. Emissions (t/h) can be estimated as given in (25).

$$E_{tot}(TG) = \sum_{i=1}^{N_{TG}} \left[\varphi_{TG_i} + (\psi_{TG_i} \times P_{TG_i}) + (\omega_{TG_i} \times {P_{TG_i}}^2) + \tau_{TG_i} \times e^{\xi_{TGi} P_{TG_i}}\right] \tag{25}$$

where φ_{TG_i}, ψ_{TG_i}, ω_{TG_i},τ_{TG_i} and ξ_{TG_i} are the coefficients of pollutant emissions related to the ith *TGs*, and are tabulated in Table 2.

3.4. Constraints

The restrictions and limitations considered while solving the OP are briefed as follows:

3.4.1. Power balance

The limitations to balance the real and reactive powers with the total load power consumed and the system network's power losses are given as follows:

$$P_{TG} = P_{L_i} + P_{Loss_i} \tag{26}$$

$$Q_{TG} = Q_{L_i} + Q_{Loss_i} \tag{27}$$

3.4.2. Bounds of the active and reactive powers

The operation bounds of the TGs, WGs, PVs, and PVHP active and reactive powers are given as follows:

$$P_{TG_i}^{min} \le P_{TG_i} \le P_{TG_i}^{max} \forall i \in N_{TG} \tag{28}$$

$$P_{WG}^{min} \le P_{WG} \le P_{WG}^{max} \tag{29}$$

$$P_{PV}^{min} \le P_{PV} \le P_{PV}^{max} \tag{30}$$

$$P_{PVHP}^{min} \le P_{PVHP} \le P_{PVHP}^{max} \tag{31}$$

$$Q_{TG_i}^{min} \le Q_{TG_i} \le Q_{TG_i}^{max} \forall i \in N_{TG} \tag{32}$$

$$Q_{WG}^{min} \le Q_{WG} \le Q_{WG}^{max} \tag{33}$$

$$Q_{PV}^{min} \le Q_{PV} \le Q_{PV}^{max} \tag{34}$$

$$Q_{PVHP}^{min} \le Q_{PVHP} \le Q_{PVHP}^{max} \tag{35}$$

3.4.3. Limits of POZs

POZs, a reason for discontinuity in the operation of the TGs, are expressed in (36):

$$P_{TG_i}^{minPOZ,j} \le POZ_{TG_i}^{j} \le P_{TG_i}^{maxPOZ,j} \tag{36}$$

where $P_{TG_i}^{minPOZ,j}$ and $P_{TG_i}^{maxPOZ,j}$ denote the minimal and maximal limits (MW) of the jth POZ of the ith TG.

3.4.4. Security limitations

The generators and load buses' permissible voltage limits are expressed in (37) and (38), respectively. Also, the thermal capacity limits are taken into account, as described in (39).

$$V_{G_i}^{min} \le V_{G_i} \le V_{G_i}^{max} \forall i \in N_G \tag{37}$$

$$V_{L_j}^{min} \le V_{L_j} \le V_{L_j}^{max} \forall j \in N_L \tag{38}$$

$$S_{L_j} \le S_{L_j}^{max} \forall j \in nl \tag{39}$$

whereV_{G_i}, V_{L_j} denote the ith's generator bus voltage and the jth's load bus voltage, respectively. N_G, N_L, and nl denote the numbers of generator buses, load buses, and branches, respectively. Another factor that quantifies the voltage quality, known as voltage deviation (VD) metric, is also considered and can be calculated as given in (40) [47].

$$VD = \left(\sum_{p=1}^{N_L} \left|V_{L_j} - 1\right|\right) \tag{40}$$

4. Optimization and decision-making techniques

4.1. IGWO

An optimization technique, that imitates the grey wolves (GWs)' social hierarchy and predatory attitude, was presented by Mirjalili in 2014 [48], and it was called the GWO technique. The GWO. The GWs are well-thought-out as the food chain's top predators. The GWO technique offers reduced parameter adjustment, easy-to-understand principles, and simplicity. In wolves' hunting policy, three significant phases are: approach, surround, and attack prey. Each gray wolf is a possible alternative in the population. The wolves in the GWO technique were split into 4 levels – level 1, denoted as α, level 2 denoted as β, level 3 denoted as δ, and level 4 denoted as ω. α is the present best individual that represents the best alternative. β andδ reflect the suboptimal second-best and third-best alternatives. Finally, ω corresponds to the ordinary alternative, so that $\alpha > \beta > \delta > \omega$. A complete explanation of this method can be found in [48]. Though, the GWO has the problem

Table 2
Cost and emission factors of the TGs [39].

Emission factors	Generators	Bus	φ_{TG} (t/h)	ψ_{TG} (t/pu. MWh)	ω_{TG} (t/pu. MW^{2}h)	τ_{TG} (t/h)	ξ_{TG} (pu. MW^{-1})
	TG_1	1	0.04091	−0.05554	0.0649	0.0002	6.667
	TG_2	2	0.02543	−0.06047	0.05638	0.0005	3.333
	TG_3	8	0.05326	−0.0355	0.0338	0.002	2
Cost factors	**Generators**	**Bus**	a_{TG} (S/h)	b_{TG} (S/MWh)	c_{TG} (S/MW^{2}h)	d_{TG} (S/h)	e_{TG} (MW^{-1})
	TG_1	1	30	2	0.00375	18	0.037
	TG_2	2	25	1.75	0.0175	16	0.038
	TG_3	8	20	3.25	0.00834	12	0.045

in realizing the global solution similar to the intelligent random-based population approaches [49–51]. To solve this problem, the improved GWO (IGWO) technique is used as follows [52]:

Surrounding: The GWs surround the prey, as expressed in (41) and (42).

$$\vec{D} = \left|\vec{C} \times \vec{X}_p(t) - \vec{X}(t)\right| \tag{41}$$

$$\vec{X}(t+1) = \vec{X}_p(t) - \vec{A} \times \vec{D} \tag{42}$$

where $\vec{X}(t)$, $\vec{X}_p(t)$, and t represent the GW's position vector, the prey position, and the tth iteration, respectively. $\vec{A}$ and $\vec{C}$ represent the vectors evaluated in (43).

$$\vec{A} = 2\vec{a}\vec{r_1} - \vec{a}, \vec{C} = 2\vec{r_2} \tag{43}$$

r_1, r_2 are random vectors ranges between 0 and 1. The elements of $\vec{a}$ are declined from 2 to 0 linearly during continual iterations as formulated in (44).

$$\vec{a} = 2 - \frac{2 \times t}{t_{max}} \tag{44}$$

Hunting: It is supposed that α, β, and δ have a better view of the prey's position. Consequently, the other wolves ω are forced to track α, β, and δ. Eq. (45) models this hunting action.

$$\overrightarrow{D_\alpha} = \left|\vec{C}_1 \times \vec{X}_\alpha - \vec{X}(t)\right|, \overrightarrow{D_\beta} = \left|\vec{C}_2 \times \vec{X}_\beta - \vec{X}(t)\right|, \text{and}$$
$$\overrightarrow{D_\delta} = \left|\vec{C}_3 \times \vec{X}_\delta - \vec{X}(t)\right| \tag{45}$$

where the coefficients $\vec{C}_1$, $\vec{C}_2$, and $\vec{C}_3$ can be determined as given in (43). The first three best solutions at the tth iteration are denoted as $\vec{X}_\alpha$, $\vec{X}_\beta$, and $\vec{X}_\delta$. Besides, the vectors $\overrightarrow{A_1}$, $\overrightarrow{A_2}$, and $\overrightarrow{A_3}$ are determined in the same way as shown in (43).

$$\overrightarrow{X_{i1}} = \vec{X}_\alpha - \overrightarrow{A_1} \times \left(\overrightarrow{D_\alpha}\right), \overrightarrow{X_{i2}} = \vec{X}_\beta - \overrightarrow{A_2} \times \left(\overrightarrow{D_\beta}\right), \text{and}$$
$$\overrightarrow{X_{i3}} = \vec{X}_\delta - \overrightarrow{A_3} \times \left(\overrightarrow{D_\delta}\right) \tag{46}$$

$$\vec{X}(t+1) = \frac{\overrightarrow{X_{i1}}(t) + \overrightarrow{X_{i2}}(t) + \overrightarrow{X_{i3}}(t)}{3} \tag{47}$$

Attacking: The hunt is ended when the prey stopovers and the wolves start attacking them. Mathematically, this can be represented by the linear decrease over the iteration's procedure controlling the diversification and intensification. Although the GWO is applicable and simple for numerous applications, the lack of population diversity, the disproportion between diversification and intensification, diversification problems (e.g., not adequate in finding a viable solution), and premature convergence [53,54] are considerable disadvantages.

Hence, to solve the ETED problem efficiently, the IGWO technique has been used in this work. Generally, there are three phases: initialization, movement, and the selection and update, which are described as follows:

Initialize the population: In this phase, N wolves are distributed randomly among the space of the search, with dimensions D, within a specified range $[l_i, u_j]$ as given in (48). In (48), t_{max} represents the maximum number of iterations.

$$\vec{X}_{ij} = l_j + rand_j[0,1] \times (u_j - l_j), i \in [1,N], j \in [1,D] \tag{48}$$

Then random initialization of the GWs' population between the boundaries of different power grid variables is performed. The ith wolf's position in the tth iteration is signified as $\vec{X}_i(t) = \left\{\overrightarrow{X_{i1}}, \overrightarrow{X_{i2}}, \cdots\cdots, \overrightarrow{X_{iD}}\right\}$. The wolves' entire population is kept in the *Pop* matrix ($N \times D$).

Movement phase: The IGWO has a motion technique called the learning-based hunting dimension (LHD) search technique. In LHD, every wolf is taught by the surrounding wolves (neighbors) to act as another candidate for $X_i(t)$'s new position. The GWO and LHD techniques produce two diverse candidates. In the LHD technique, the dimension of the location of the wolf $\vec{X}_i(t)$ is evaluated where each wolf can learn by its various neighbors, in addition to another wolf from *Pop* selected randomly. Besides $\vec{X}_{i\text{-}GWO}(t+1)$, the LHD technique creates another candidate, named $\vec{X}_{i-LHD}(t+1)$, for the new position. To do so, a radius $\vec{R}_i(t)$ is evaluated by calculating the Euclidean distance from $\vec{X}_i(t)$ to the position candidate's $\vec{X}_{i\text{-}GWO}(t+1)$, as shown in (49).

$$\vec{R}_i(t) = \|\vec{X}_i(t) - \vec{X}_{i-GWO}(t+1)\| \tag{49}$$

At that point, the surrounding neighbors of $\vec{X}_i(t)$, represented by $\vec{N}_i(t)$, can be made by (50) concerning radius $\vec{R}_i(t)$, where $\vec{D}_i$ represents the Euclidean distance between $\vec{X}_i(t)$ and $\vec{X}_j(t)$. Further, multi neighbors learning is represented by (51) whenever the neighborhood of $\vec{X}_i(t)$ is built.

$$\vec{N}_i(t) = \left\{\vec{X}_j(t) \middle| \vec{D}_i\left(\vec{X}_i(t), \vec{X}_j(t)\right) \le \vec{R}_i(t), \vec{X}_j(t) \in Pop\right\} \tag{50}$$

The dth dimension of $\vec{X}_{i-LHD,d}(t+1)$ can be determined by utilizing the dth dimension of a random neighbor $\vec{X}_{n,d}(t)$ chosen from $\vec{N}_i(t)$and any randomly selected wolf $\vec{X}_{r,d}(t)$ from *Pop*.

$$\vec{X}_{i-LHD,d}(t+1) = \vec{X}_{i,d}(t) + rand \times \left(\vec{X}_{n,d}(t) - \vec{X}_{r,d}(t)\right) \tag{51}$$

Select and update the GWs' locations: This phase indicates surrounding and attacking the prey. The candidate who scored the best fitness is nominated through comparisons of the fitness values of the candidates $\vec{X}_{i\text{-}GWO}(t+1)$ and $\vec{X}_{i-LHD,d}(t+1)$, as shown in (52). Once the prey has been surrounded, the GWs $\alpha, \beta,$ and δ better understood the possible prey's location.

$$\vec{X}_i(t+1) = \begin{cases} \vec{X}_{i-GWO}(t+1), iff(\vec{X}_{i-GWO}) < f(\vec{X}_{i-LHD}) \\ \vec{X}_{i-LHD}(t+1) otherwise \end{cases} \tag{52}$$

Then, to upgrade the process to the new location named $\vec{X}_i(t+1)$, we have two conditions – if the fitness value of the chosen candidate is less than $\vec{X}_i(t)$ then $\vec{X}_i(t)$ is upgraded by the chosen candidate, or $\vec{X}_i(t)$ keeps as it is in the *Pop* matrix. Finally, the iterations' counter (*iter*) is increased until t_{max} is reached. The flowchart of the IGWO technique is shown in Fig. 5.

4.2. Analytic hierarchy process (AHP)

When the multiplicity of engineering issues increases, the SO investigation is no longer an outstanding alternative because of the objectives' trade-off. i.e., enhancing the objective value of a design may reduce other objectives' performance, especially when many options are available [55,56]. Indeed, MO problems and methods can be used. However, they are not enough to provide many optimal points on the Pareto curve that satisfy the decision-makers' needs, especially with tri-or quad-objectives. This means that we can sometimes allow the decision-maker to arrive at one of the Pareto issues that are the most natural to look at all matters of interest repeatedly. Among the numerous procedures with several parameters and several characteristics, AHP is one of the most used methods in decision-making, and it is providing several benefits: simplicity, adaptability, and clarity that allow for comparing and assessing different alternatives. In most

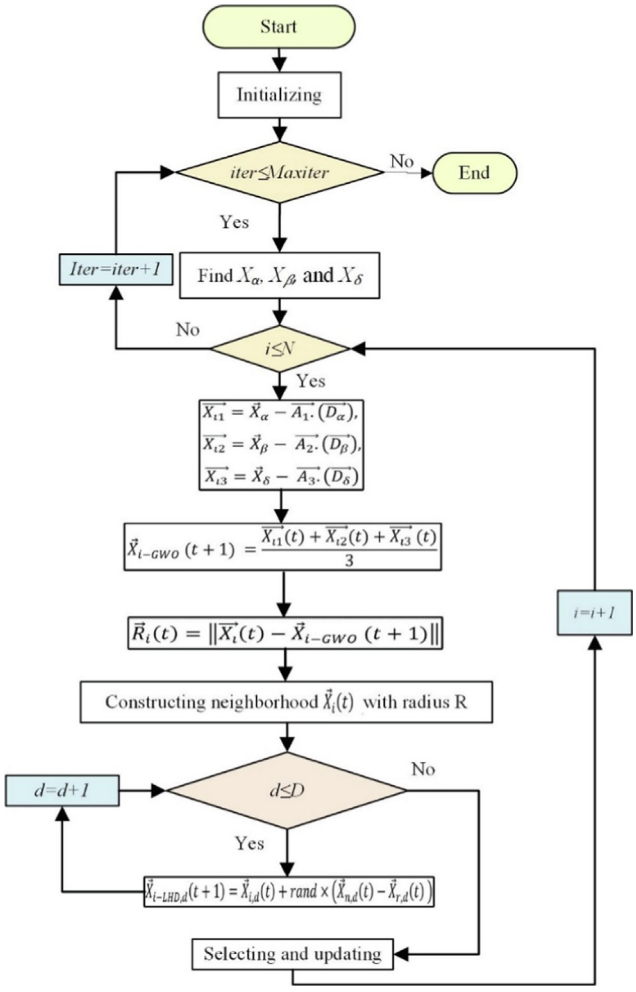

Fig. 5. The flowchart of the IGWO technique.

instances, it is the primary way to find the most viable approach to implement a prioritizing scheme. It also has some drawbacks, such as the interdependence between priorities and choices and the need to assign weights (pairwise comparisons), based on data available, to determine which preference should be favored by designers [57,58].

To create a decision matrix (judgment), the AHP method relies on pairwise comparison of the various attributes. At that point, this matrix's maximum eigenvalue is utilized for weighing the attributes [59,60]. AHP has been recently used in numerous applications of the power grid. Wang et al. [61] have utilized this to obtain the best locations of solar power plants for seeking of energy planning aspects. Dehghanian et al. [62] have proposed a fuzzy-based AHP framework to determine the optimal prioritized maintenance of reliable power system components. Abdel Aleem et al. [63] have used AHP for choosing multiple credits of energy in green energy standard codes to realize the optimal energy credits that meet the Egyptian standard needs. Elbasuony et al. [64] presented AHP for weighing different power quality indices for numerous interface buses in the distributed generation schemes. In accordance, AHP is exploited to quantify the weights of fuel costs, losses, and emission levels. The typical AHP method is summarized as [57] – build a model of hierarchy; form the matrix of judgment; evaluate the maximum eigenvalue (λ_{max}) and the respective eigenvector of the judgment, in which the eigenvector elements should reflect the relative weights of the relative factor, so-called "hierarchical ranking"; and finally, verify the accuracy of the AHP by the consistency index (CI), as follows:

$$CI = \frac{\lambda_{max} - N_j}{N_j - 1} \tag{53}$$

Besides, estimate the consistency ratio (CR), as follows:

$$CR = \frac{CI}{RI} \tag{54}$$

N_j and RI represent the dimension of the judgment matrix and the average stochastic CI that relies on this matrix.

The pairwise comparison relies on a fundamental scale ranges from 1 to 9, in which Scale 1: demonstrates the equality criterion, Scale 3 demonstrates a marginally higher significant measure compared to the other one, Scale 5 indicates that one measure is more significant than the other, Scale 7 suggests that one measure is much significant than the other, and finally Scale 9 means that one criterion is highly significant than the other one. Fig. 6 shows an illustrative flowchart for the AHP implementation procedure. More information about AHP can be found in [65].

5. Simulation results

Five scenarios are addressed. In Scenario I, only fuel costs are minimized. In Scenario II, only power losses are considered to be minimized. Besides, in Scenario III, only emissions levels are considered to be minimized. The first three scenarios represent a SO optimization formulation. The results obtained from the first three scenarios are used in the rest of the weighted sum-based scenarios as the base values to have comparable goals, not to realize a biased

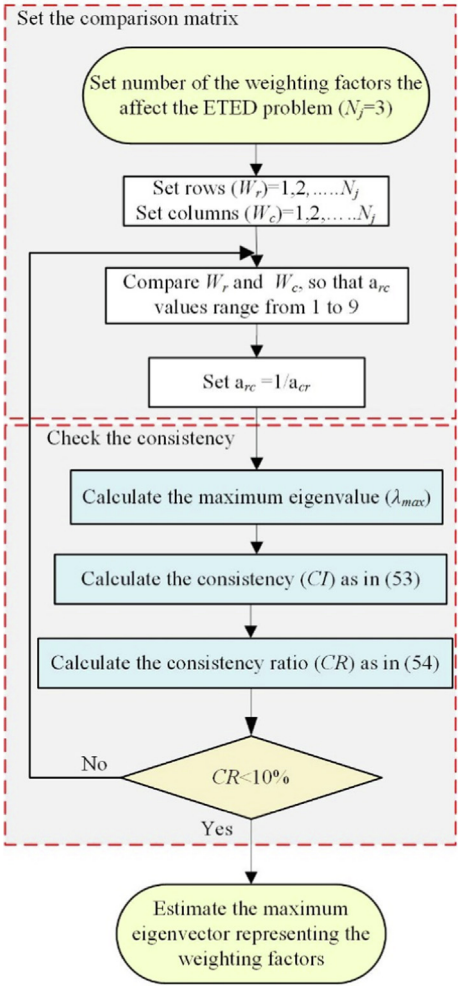

Fig. 6. The flowchart for the AHP implementation procedure.

Table 3
Results obtained for fuel costs minimization (the value given in bold indicates the best result got).

Variables and parameters		Min	Max	MFO	SSA	IGWO	MVO
Active power (MW)	P_{TG1}	50	140	152.05429	151.24668	150.04408	152.31199
	P_{TG2}	20	80	42.57366	42.84803	43.48963	42.04944
	P_{TG3}	10	35	10.00000	10.08840	10.02458	10.07894
Reactive power (MVAr)	Q_1	−50	140	−11.36590	−11.94310	−11.03505	−14.77419
	Q_2	−20	60	21.86743	14.35066	21.40220	14.80141
	Q_5	−15	40	25.95090	35.00000	25.86958	35.00000
	Q_8	−30	35	40.00000	40.00000	40.00000	40.00000
	Q_{11}	−20	25	20.85680	20.19068	21.00448	19.18328
	Q_{13}	−20	25	22.28300	21.33422	22.27803	25.00000
Bus voltage (pu)	V_1	0.96	1.10	1.07637	1.07738	1.07664	1.07869
	V_2	0.96	1.10	1.07011	1.07137	1.07044	1.07306
	V_5	0.96	1.10	1.06356	1.06459	1.06367	1.06652
	V_8	0.96	1.10	1.04268	1.04297	1.04278	1.04903
	V_{11}	0.96	1.10	1.03992	1.04070	1.04018	1.04444
	V_{13}	0.96	1.10	1.02590	1.02659	1.02614	1.03090
P_{loss} (MW)		Not applicable		6.6551	6.5942	6.5258	6.6816
VD (pu)				0.94580	0.97531	0.95113	1.05693
$W_{gencost}$				126.9591	137.2552	125.8858	127.1258
$S_{gencost}$				114.9636	109.5690	123.5391	110.6119
Sh_{gencost}				39.9283	39.4895	39.5998	39.6447
Total cost ($/MWh)				812.4878	812.5615	**811.8384**	812.5497
Emission (t/h)				5.22541	5.32013	4.58865	5.31307
$Fuel_{vlvcost}$				553.1386	547.9629	543.8264	558.3788
Computation time (s)				333.063019	548.202445	320.798879	415.978702

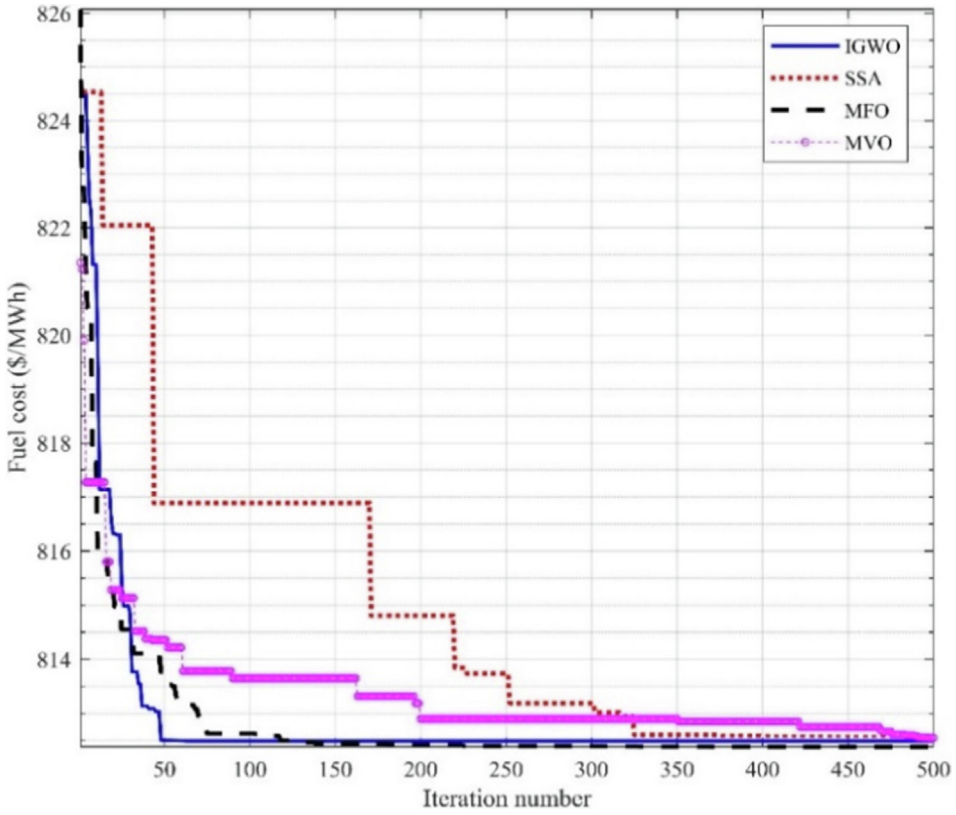

Fig. 7. Convergence curve of total fuel costs.

solution. The weighted sum approach, one of the most widely used methods due to its simplicity, was used to convert the problem into a scalar normalized one by constructing a weighted sum of all the objectives in Scenarios IV and V. In Scenario IV, all the objective functions are considered to be minimized with equal weighting factors. Afterward, in Scenario V, all the objectives are minimized while using the weighting factors obtained from the AHP. The three RESs considered in this work are kept connected to buses 5, 11, and 13 in all the schemes under investigation.

5.1. Scenario I

The total fuel cost is minimized as the primary target in the ETED problem. The variables obtained via the proposed IGWO are

Table 4
Results obtained for power losses minimization (the value given in bold indicates the best result got).

Variables and parameters		Min	Max	MFO	SSA	IGWO	MVO
Active power (MW)	P_{TG1}	50	140	34.65845	34.77954	34.65974	34.84796
	P_{TG2}	20	80	80.00000	79.97559	79.99980	79.98132
	P_{TG3}	10	35	35.00000	34.99488	34.99922	34.99599
Reactive power (MVAr)	Q_1	−50	140	−5.84144	−5.83250	−5.88264	−6.59519
	Q_2	−20	60	12.85196	12.79827	12.98597	11.94761
	Q_5	−15	40	22.89116	22.89046	22.83186	23.75420
	Q_8	−30	35	40.00000	40.00000	40.00000	40.00000
	Q_{11}	−20	25	18.34947	18.33382	18.36013	17.94969
	Q_{13}	−20	25	18.73407	18.79553	18.69136	19.86471
Bus voltage (pu)	V_1	0.96	1.10	1.08695	1.08695	1.08694	1.08752
	V_2	0.96	1.10	1.08320	1.08320	1.08319	1.08391
	V_5	0.96	1.10	1.07133	1.07133	1.07131	1.07208
	V_8	0.96	1.10	1.04873	1.04880	1.04866	1.05080
	V_{11}	0.96	1.10	1.04897	1.04900	1.04893	1.05031
	V_{13}	0.96	1.10	1.03458	1.03462	1.03453	1.03610
P_{loss} (MW)		Not applicable		2.3584	2.3607	**2.3584**	2.3599
VD (pu)				1.19990	1.20042	1.19901	1.23027
$W_{gencost}$				258.7630	258.5885	258.7629	258.7630
$S_{gencost}$				180.7632	182.4142	181.2130	181.1290
Sh_{gencost}				40.0073	39.9858	39.9416	39.9742
Total cost ($/MWh)				929.3213	930.9195	929.7045	929.3172
Emission (t/h)				0.10081	0.10080	0.10081	0.10072
$Fuel_{vlvcost}$				482.4348	482.5182	482.4329	482.0177
Computation time (s)				505.153871	282.945590	218.322438	320.935911

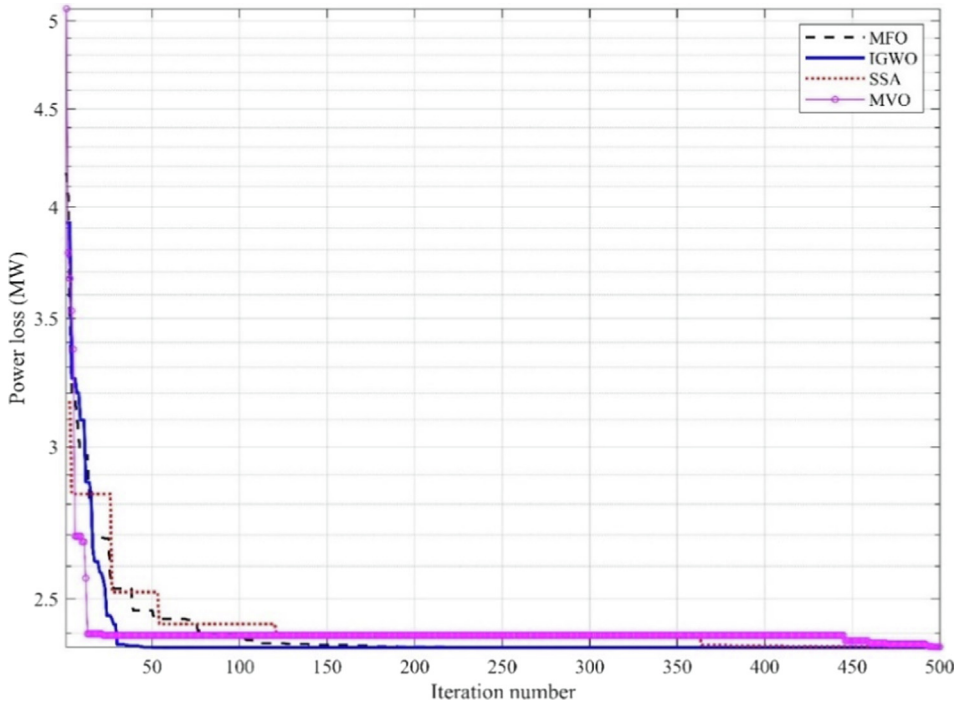

Fig. 8. Convergence curve of power losses for the proposed system.

compared to the three optimizers under consideration, as presented in Table 3. Notably, a minimum cost of 811.8384 $/MWh is obtained via the proposed IGWO with a minimum power loss of 6.5258 MW. The convergence curve of the fitness value using the proposed IGWO and the other optimization algorithms is explored in Fig. 7. Besides, the IGWO obtained the solution quickly (computational time is around 320.798879 s) compared to the others, followed by the MFO algorithm (computational time is around 333.063019 s).

5.2. Scenario II

The power loss is minimized as the secondary target in the ETED problem. Also, the results obtained via IGWO compared to the three optimizers under consideration, as shown in Table 4. It is clear that a minimum power loss of 2.3584 MW is obtained via the proposed IGWO. The convergence curve of power losses using the proposed IGWO and the three other optimization algorithms is displayed in Fig. 8. Notably, the IGWO obtained the solu-

Table 5
Results obtained for emissions level minimization (the value given in bold indicates the best result got).

Variables and parameters		Min	Max	MFO	SSA	IGWO	MVO
Active power (MW)	P_{TG1}	50	140	46.09349	46.63642	46.10721	46.07680
	P_{TG2}	20	80	68.62327	68.08430	68.60972	68.58460
	P_{TG3}	10	35	35.00000	34.99999	35.00000	35.00000
Reactive power (MVAr)	Q_1	−50	140	−5.80643	−5.05471	−5.80472	−6.25551
	Q_2	−20	60	12.79751	12.64142	13.11927	18.19664
	Q_5	−15	40	22.82677	22.95064	22.87455	19.93807
	Q_8	−30	35	40.00000	40.00000	40.00000	40.00000
	Q_{11}	−20	25	18.71174	19.02737	18.81927	19.52001
	Q_{13}	−20	25	18.75256	17.78522	18.28744	16.03859
Bus voltage (pu)	V_1	0.96	1.10	1.08615	1.08568	1.08602	1.08515
	V_2	0.96	1.10	1.08219	1.08161	1.08204	1.08097
	V_5	0.96	1.10	1.07065	1.07005	1.07044	1.06912
	V_8	0.96	1.10	1.04784	1.04610	1.04712	1.04324
	V_{11}	0.96	1.10	1.04813	1.04704	1.04771	1.04527
	V_{13}	0.96	1.10	1.03371	1.03246	1.03322	1.03042
P_{loss} (MW)		Not applicable		2.4168	2.4207	2.4169	2.4221
VD (pu)				1.17750	1.15302	1.16851	1.11358
$W_{gencost}$				258.7630	258.7629	258.7629	258.7279
$S_{gencost}$				180.9240	181.3282	181.2447	182.2155
Sh_{gencost}				39.9797	39.9969	39.9316	39.9815
Total cost ($/MWh)				906.2883	905.7517	906.5368	907.7137
Emission (t/h)				0.09783	0.097838	**0.09783**	0.097832
$Fuel_{vlvcost}$				455.4321	454.2022	455.4013	455.5634
Computation time (s)				541.508718	312.305162	209.162713	283.680463

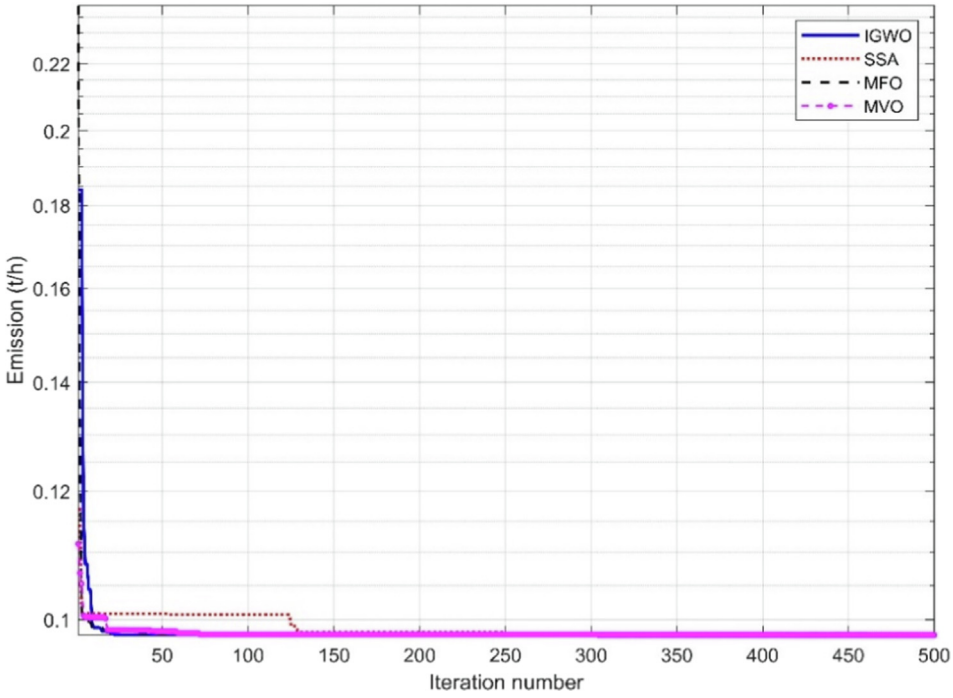

Fig. 9. Convergence curve of emission levels for the proposed system.

tion quickly (computational time is around 218.322438 s) than the others, followed by the SSA technique (computational time is around 282.945590 s).

5.3. Scenario III

The pollutant emissions level is minimized as the third target applied to the system. The obtained results via the proposed IGWO compared to the three optimizers under consideration, as shown in Table 5. It is clear that a minimum emissions level of 0.09783 t/h is obtained via the proposed IGWO with a power loss of 2.4169 MW within 209.163 s. The convergence curve of emissions level using the proposed IGWO and the other optimizations is shown in Fig. 9.

5.4. Scenario IV

The three objectives are minimized simultaneously with equal weighting factors (i.e., w_1, w_2, and $w_3 = 0.333$). The three best results, given in bold in Tables 3–5, are used to normalize the objective functions. Then, the proposed IGWO technique is applied to minimize the three objectives of the system. The variables obtained via IGWO are also compared to the other optimizers, as

Table 6
Results obtained for equal weights MO optimization.

Variables and parameters		Min	Max	MFO	SSA	IGWO	MVO
Active power (MW)	P_{TG1}	50	140	45.18172	40.04290	45.20047	44.09031
	P_{TG2}	20	80	69.52915	74.67228	69.51062	70.64390
	P_{TG3}	10	35	35.00000	34.99321	35.00000	35.00000
Reactive power (MVAr)	Q_1	−50	140	−5.80929	−5.80569	−5.83193	−2.98461
	Q_2	−20	60	12.79842	12.77381	12.82590	11.21679
	Q_5	−15	40	22.83176	22.85632	22.83534	21.96548
	Q_8	−30	35	40.00000	40.00000	40.00000	40.00000
	Q_{11}	−20	25	18.68309	18.51650	18.68305	19.05723
	Q_{13}	−20	25	18.75073	18.77337	18.74239	18.10271
Bus voltage (pu)	V_1	0.96	1.10	1.08621	1.08657	1.08621	1.08532
	V_2	0.96	1.10	1.08227	1.08272	1.08227	1.08117
	V_5	0.96	1.10	1.07070	1.07101	1.07070	1.06965
	V_8	0.96	1.10	1.04791	1.04834	1.04790	1.04600
	V_{11}	0.96	1.10	1.04820	1.04859	1.04820	1.04674
	V_{13}	0.96	1.10	1.03378	1.03419	1.03378	1.03220
P_{loss} (MW)		Not applicable		2.4109	2.3824	2.4110	2.4068
VD (pu)				1.17927	1.18952	1.17923	1.14439
$W_{gencost}$				258.7630	258.7315	258.7629	258.7193
$S_{gencost}$				179.6436	180.8166	181.5155	182.0602
Sh_{gencost}				39.9320	39.9835	39.9389	39.9088
Total cost ($/MWh)				906.6000	917.8263	908.4451	911.0870
Emission (t/h)				0.09785	0.09870	0.09785	0.09794
Total objective				1.0453	1.0488	**1.0461**	1.0467
$Fuel_{vlvcost}$				457.5116	469.5920	457.4691	460.1401
Computation time (s)				159.874675	217.963439	385.008094	223.746449

presented in Table 6. The convergence curve is displayed in Fig. 10. Notably, a minimum objective of 1.0461 pu is obtained via the IGWO within a computational time of 385.008094 s.

5.5. Scenario V

In this scenario, the objectives were arranged according to their importance to the decision-maker. Based on the perspective of power utilities in Egypt, the voltage's quality is the priority, and it should comply with the national standards. Reducing fuel costs comes as the first priority of network operators in the current phase. Then, active power loss reduction comes as the secondary goal. Despite the importance of lowering the emission levels, they are classified as the third-priority. However, the pair-wise comparison used to formulate the AHP can be modified to meet other perspectives. In sequence, the judgment matrix of this scenario is specified, as shown in Table 7. Clearly, the suggested assessment maintains its consistency, in which: λ_{max}= 3.0111, RI = 0.58, and CR = 1% <10% (which indicates acceptable CR percent). The calculated weights of fuel costs, power losses, and emission levels using the AHP are 0.5393, 0.2974, and 0.1633, respectively.

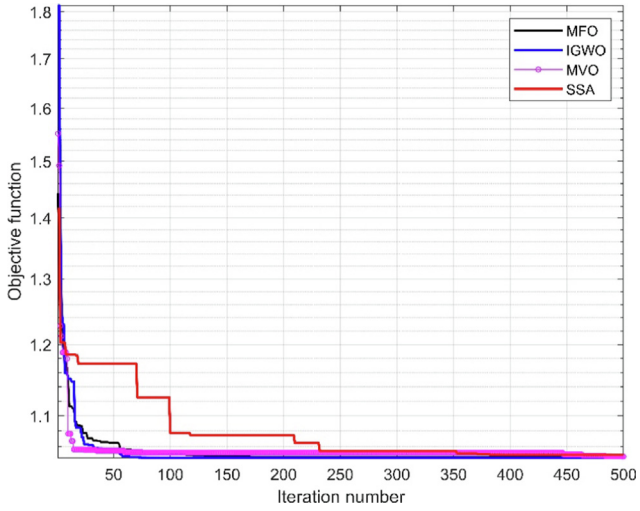

Fig. 10. Convergence curve for equal weights MO optimization of the proposed system.

Table 7
Judgment matrix of Scenario V.

Objectives	Fuel costs	Losses	Emissions
Fuel costs	1/1	2/1	3/1
Losses	1/2	1/1	2/1
Emissions	1/3	1/2	1/1

Four optimization techniques are applied to minimize the AHP-based objective. The variables obtained via IGWO are also compared to the other optimizers, as shown in Table 8. The convergence curve is displayed in Fig. 11. A minimum objective of 1.0699 pu is obtained via the proposed IGWO within a computational time of 169.8182 s.

Table 9 shows a comparative analysis of different optimization techniques in the literature and the proposed IGWO with AHP. Remarkably, the results obtained using the proposed IGWO-AHP are compared to the corresponding results obtained using SMODE [39], MOEA/D [27], MODA [66], MOFA-CPA [67], PSO-SSO [21], and MVO [68]. The AHP-ETED model presented in this work can significantly minimize fuel costs to 902.4951 $/h, lower emission levels as 0.09785 t/h, and achieve a lower power loss of 2.4110 MW. The results attained validate that the IGWO outperforms the other considered algorithms in finding the best solution to the ETED problem.

Fig. 12 shows a comparison of the considered optimizers' values for fuel cost, power loss, and emissions, respectively. It can be seen that the AHP-based approach (Scenario V) achieved the best fuel cost value compared to the equal weight-based approach (Scenario IV); however, both scenarios almost realized the same power losses and emissions values. In comparison with the other addressed optimization techniques, it can be seen that the proposed scenarios (Scenarios IV and V) achieve better power losses and emissions values. But with relatively higher fuel costs.

Table 8
Results obtained via IGWO for AHP-based objective minimization.

Variables and parameters		Min	Max	MFO	SSA	IGWO	MVO
Active power (MW)	P_{TG1}	50	140	48.55312	38.67082	48.51921	48.54658
	P_{TG2}	20	80	66.18098	77.15253	66.21427	66.39000
	P_{TG3}	10	35	35.00000	33.92502	35.00000	35.00000
Reactive power (MVAr)	Q_1	−50	140	−5.89415	−5.85001	−5.79898	−8.40780
	Q_2	−20	60	12.61675	12.97551	12.79831	14.70985
	Q_5	−15	40	23.06820	22.88073	22.81347	23.72562
	Q_8	−30	35	40.00000	40.00000	40.00000	40.00000
	Q_{11}	−20	25	18.74765	18.55917	18.78776	18.44905
	Q_{13}	−20	25	18.81138	18.60636	18.75773	18.85749
Bus voltage (pu)	V_1	0.96	1.10	1.08604	1.08653	1.08598	1.08634
	V_2	0.96	1.10	1.08206	1.08268	1.08198	1.08251
	V_5	0.96	1.10	1.07058	1.07092	1.07050	1.07081
	V_8	0.96	1.10	1.04780	1.04808	1.04765	1.04821
	V_{11}	0.96	1.10	1.04807	1.04843	1.04796	1.04843
	V_{13}	0.96	1.10	1.03365	1.03400	1.03353	1.03403
P_{loss} (MW)		Not applicable		2.4338	2.3986	2.4335	2.4411
VD (pu)				1.17556	1.18605	1.17280	1.18611
$W_{gencost}$				258.7628	258.6994	258.7630	258.6838
$S_{gencost}$				181.4209	182.3227	181.2091	182.0296
Sh_{gencost}				39.9266	39.9132	40.0895	39.7836
Total cost ($/MWh)				902.4886	922.9256	902.4951	903.7106
Emission (t/h)				0.09798	0.09970	0.09798	0.09804
Total objective				1.07	1.082	**1.0699**	1.0715
$Fuel_{vlvcost}$				449.8984	473.0772	449.9725	450.7142
Computation time (s)				390.239344	237.966138	169.818209	228.678605

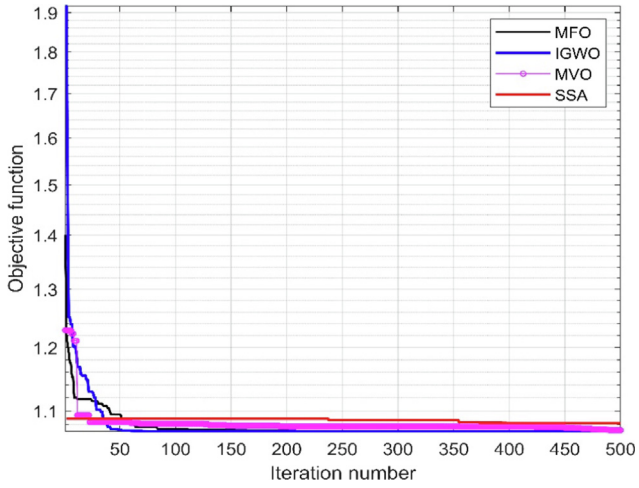

Fig. 11. Convergence curve of total objective for the proposed system using AHP.

6. Conclusions

This paper presents a MO-ETED problem for obtaining the best compromise solutions, total costs, losses, and emissions of a modified IEEE 30-bus comprised thermal and RESs such as wind, PV, and PVHP. The main goal is to minimize the total fuel costs, active power losses, and emission levels. Different equality and inequality limits involving POZs were considered as system restrictions. Metaheuristic optimization techniques – MFO, SSA, IGWO, and MVO – were employed to find the best solutions. Various scenarios are examined to verify the potential of the suggested model in solving the OP. AHP was effectively utilized in quantifying the weights of the ETED problem. Finally, the results obtained validate that the IGWO outperforms the other considered algorithms in solving the ETED problem. The ETED formulation may be widely studied further by using other optimization algorithms, particularly the hybrid algorithms. Besides, the non-convex ETED issue and uncertainty in load demands over a time-period incorporated with uncertainties of all RESs remain a challenge to be investigated in possible future work.

Declaration of Competing Interest

The authors declare that they have no known competing financial interests or personal relationships that could have appeared to influence the work reported in this paper.

Acknowledgments

This research was funded by the Deanship of Scientific Research (DSR) at King Abdulaziz University, Jeddah, under grant no. (RG-21-135-39). The authors, therefore, acknowledge with thanks to DSR technical and financial support.

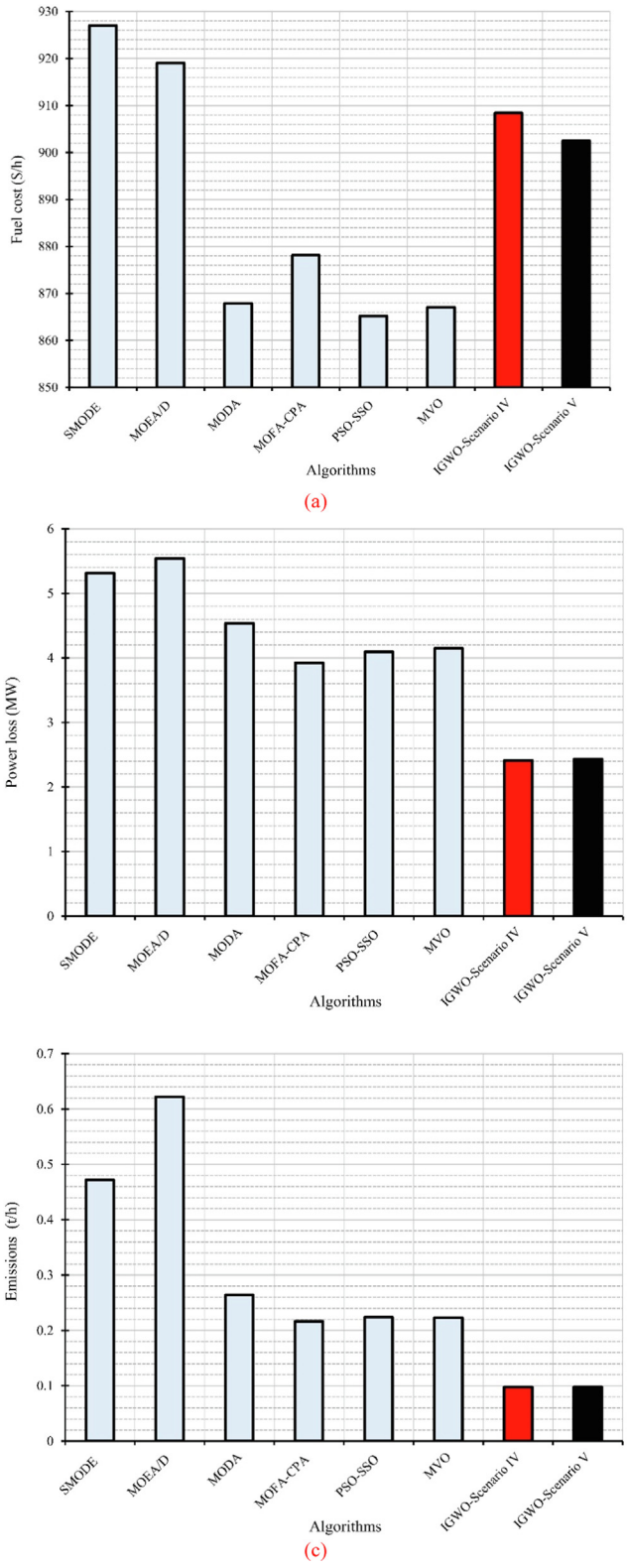

Fig. 12. Comparison of the values obtained using the considered optimizers: (a) Fuel cost, (b) Power loss, and (c) Emissions.

Table 9
The comparative analysis by using different optimization techniques.

Objectives	SMODE	MOEA/D	MODA	MOFA-CPA	PSO-SSO	MVO	Proposed IGWO	
	[39]	[27]	[66]	[67]	[21]	[68]	Equal weights	AHP- weights
Fuel cost ($/h)	927.049	919.040	867.9070	878.13	865.18	867.034	908.4451	902.4951
Power loss (MW)	5.3148	5.5429	4.5342	3.9232	4.093	4.148	2.4110	2.4335
Emissions (t/h)	0.4721	0.6221	0.2640	0.2165	0.224	0.223	0.09785	0.09798

Table A1
Direct, reserve, and standby cost coefficients.

Cost coefficients ($/MW)	WG (bus 5)	PV (bus 11)	PVHP (bus 13)
Direct	$K_{d_{WG}}$ = 1.7	$K_{d_{PV}}$ = 1.6	$K_{d_{PVHP}}$ = 1.5
Reserve	$K_{r_{WG}}$ = 3.0	$K_{r_{PV}}$ = 3.0	$K_{r_{PVHP}}$ = 3.0
Penalty	$K_{s_{WG}}$ = 1.4	$K_{s_{PV}}$ = 1.4	$K_{s_{PVHP}}$ = 1.4

Appendix A

Table A1 shows the values of the cost coefficients of the stochastic RESs.

References

[1] Secui DC. Large-scale multi-area economic/emission dispatch based on a new symbiotic organisms search algorithm. Energy Convers Manag 2017;154:203–23. doi: https://doi.org/10.1016/j.enconman.2017.09.075.
[2] Omar AI, Ali ZM, Al-Gabalawy M, Abdel Aleem SHEE, Al-Dhaifallah M. Multi-objective environmental economic dispatch of an electricity system considering integrated natural gas units and variable renewable energy sources. Mathematics 2020;8:1100. doi: https://doi.org/10.3390/math8071100.
[3] Xiong G, Shi D. Orthogonal learning competitive swarm optimizer for economic dispatch problems. Appl Soft Comput 2018;66:134–48. doi: https://doi.org/10.1016/j.asoc.2018.02.019.
[4] Abdelaziz AY, Ali ES, Abd Elazim SM. Flower pollination algorithm to solve combined economic and emission dispatch problems. Eng Sci Technol an Int J 2016;19:980–90. doi: https://doi.org/10.1016/j.jestch.2015.11.005.
[5] Rizk-Allah RM, Abdel Mageed HM, El-Sehiemy RA, Abdel Aleem SHE, El Shahat A. A new sine cosine optimization algorithm for solving combined non-convex economic and emission power dispatch problems. Int J Energy Convers 2017;5:180. doi: https://doi.org/10.15866/irecon.v5i6.14291.
[6] McLarty D, Panossian N, Jabbari F, Traverso A. Dynamic economic dispatch using complementary quadratic programming. Energy 2019;166:755–64. doi: https://doi.org/10.1016/j.energy.2018.10.087.
[7] Zhan JP, Wu QH, Guo CX, Zhou XX. Fast λ-iteration method for economic dispatch with prohibited operating zones. IEEE Trans Power Syst 2014;29:990–1. doi: https://doi.org/10.1109/TPWRS.2013.2287995.
[8] Elsheakh Y, Zou S, Ma Z, Zhang B. Decentralised gradient projection method for economic dispatch problem with valve point effect. IET Gener Transm Distrib 2018;12:3844–51. doi: https://doi.org/10.1049/iet-gtd.2018.0369.
[9] Mahdi FP, Vasant P, Kallimani V, Watada J, Fai PYS, Abdullah-Al-Wadud M. A holistic review on optimization strategies for combined economic emission dispatch problem. Renew Sustain Energy Rev 2018;81:3006–20. doi: https://doi.org/10.1016/j.rser.2017.06.111.
[10] Wang MQ, Gooi HB, Chen SX, Lu S. A mixed integer quadratic programming for dynamic economic dispatch with valve point effect. IEEE Trans Power Syst 2014;29:2097–106. doi: https://doi.org/10.1109/TPWRS.2014.2306933.
[11] Pan S, Jian J, Chen H, Yang L. A full mixed-integer linear programming formulation for economic dispatch with valve-point effects, transmission loss and prohibited operating zones. Electr Power Syst Res 2020;180:. doi: https://doi.org/10.1016/j.epsr.2019.106061106061.
[12] Chen F, Huang GH, Fan YR, Liao RF. A nonlinear fractional programming approach for environmental–economic power dispatch. Int J Electr Power Energy Syst 2016;78:463–9. doi: https://doi.org/10.1016/j.ijepes.2015.11.118.
[13] Pan S, Jian J, Yang L. A hybrid MILP and IPM approach for dynamic economic dispatch with valve-point effects. Int J Electr Power Energy Syst 2018;97:290–8. doi: https://doi.org/10.1016/j.ijepes.2017.11.004.
[14] El-Fergany AA, Hasanien HM. Single and multi-objective optimal power flow using grey wolf optimizer and differential evolution algorithms. Electr Power Components Syst 2015;43:1548–59. doi: https://doi.org/10.1080/15325008.2015.1041625.
[15] Susowake Y, Masrur H, Yabiku T, Senjyu T, Howlader AM, Abdel-Akher M, et al. A multi-objective optimization approach towards a proposed smart apartment with demand-response in Japan. Energies 2019;13:127. doi: https://doi.org/10.3390/en13010127.
[16] Elsakaan AA, El-Sehiemy RA, Kaddah SS, Elsaid MI. An enhanced moth-flame optimizer for solving non-smooth economic dispatch problems with emissions. Energy 2018;157:1063–78. doi: https://doi.org/10.1016/j.energy.2018.06.088.
[17] Medani K ben oualid, Sayah S, Bekrar A. Whale optimization algorithm based optimal reactive power dispatch: A case study of the Algerian power system. Electr Power Syst Res 2018;163:696–705. doi:10.1016/j.epsr.2017.09.001.
[18] Nourianfar H, Abdi H. Solving the multi-objective economic emission dispatch problems using fast non-dominated sorting TVAC-PSO combined with EMA. Appl Soft Comput J 2019;85:. doi: https://doi.org/10.1016/j.asoc.2019.105770105770.
[19] Mason K, Duggan J, Howley E. Multi-objective dynamic economic emission dispatch using particle swarm optimisation variants. Neurocomputing 2017;270:188–97. doi: https://doi.org/10.1016/j.neucom.2017.03.086.
[20] Karthik N, Parvathy AK, Arul R. Multi-objective economic emission dispatch using interior search algorithm. Int Trans Electr Energy Syst 2019;29:. doi: https://doi.org/10.1002/etep.2683e2683.
[21] El Sehiemy RA, Selim F, Bentouati B, Abido MA. A novel multi-objective hybrid particle swarm and salp optimization algorithm for technical-economical-environmental operation in power systems. Energy 2020;193:. doi: https://doi.org/10.1016/j.energy.2019.116817116817.
[22] Ding M, Chen H, Lin N, Jing S, Liu F, Liang X, et al. Dynamic population artificial bee colony algorithm for multi-objective optimal power flow. Saudi J Biol Sci 2017;24:703–10. doi: https://doi.org/10.1016/j.sjbs.2017.01.045.
[23] Liang RH, Wu CY, Chen YT, Tseng WT. Multi-objective dynamic optimal power flow using improved artificial bee colony algorithm based on Pareto optimization. Int Trans Electr Energy Syst 2016;26:692–712. doi: https://doi.org/10.1002/etep.2101.
[24] Wang G, Zha Y, Wu T, Qiu J, Peng J, Xu G. Cross entropy optimization based on decomposition for multi-objective economic emission dispatch considering renewable energy generation uncertainties. Energy 2020;193:. doi: https://doi.org/10.1016/j.energy.2019.116790116790.
[25] Chen MR, Zeng GQ, Di Lu K. Constrained multi-objective population extremal optimization based economic-emission dispatch incorporating renewable energy resources. Renew Energy 2019;143:277–94. doi: https://doi.org/10.1016/j.renene.2019.05.024.
[26] Biswas PP, Suganthan PN, Qu BY, Amaratunga GAJ. Multiobjective economic-environmental power dispatch with stochastic wind-solar-small hydro power. Energy 2018;150:1039–57. doi: https://doi.org/10.1016/j.energy.2018.03.002.
[27] Biswas PP, Suganthan PN, Mallipeddi R, Amaratunga GAJ. Multi-objective optimal power flow solutions using a constraint handling technique of evolutionary algorithms. Soft Comput 2020;24:2999–3023. doi: https://doi.org/10.1007/s00500-019-04077-1.
[28] Bora TC, Mariani VC, Coelho L dos S. Multi-objective optimization of the environmental-economic dispatch with reinforcement learning based on non-dominated sorting genetic algorithm. Appl Therm Eng 2019;146:688–700. doi:10.1016/j.applthermaleng.2018.10.020.
[29] Yin Y, Liu T, He C. Day-ahead stochastic coordinated scheduling for thermal-hydro-wind-photovoltaic systems. Energy 2019;187:. doi: https://doi.org/10.1016/j.energy.2019.115944115944.
[30] Li X, Wang W, Wang H, Wu J, Fan X, Xu Q. Dynamic environmental economic dispatch of hybrid renewable energy systems based on tradable green certificates. Energy 2020;193:. doi: https://doi.org/10.1016/j.energy.2019.116699116699.
[31] Elattar EE. Environmental economic dispatch with heat optimization in the presence of renewable energy based on modified shuffle frog leaping algorithm. Energy 2019;171:256–69. doi: https://doi.org/10.1016/j.energy.2019.01.010.
[32] Saleh AA, Senjyu T, Alkhalaf S, Alotaibi MA, Hemeida AM. Water cycle algorithm for probabilistic planning of renewable energy resource, considering different load models. Energies 2020;13:5800. doi: https://doi.org/10.3390/en13215800.
[33] Gamil MM, Sugimura M, Nakadomari A, Senjyu T, Howlader HOR, Takahashi H, et al. Optimal sizing of a real remote Japanese microgrid with sea water electrolysis plant under time-based demand response programs. Energies 2020;13. doi: https://doi.org/10.3390/en13143666.
[34] Modiri-Delshad M, Rahim NA. Multi-objective backtracking search algorithm for economic emission dispatch problem. Appl Soft Comput 2016;40:479–94. doi: https://doi.org/10.1016/j.asoc.2015.11.020.
[35] Howlader HOR, Adewuyi OB, Hong Y-Y, Mandal P, Mohamed Hemeida A, Senjyu T. Energy storage system analysis review for optimal unit commitment. Energies 2019;13:158. doi: https://doi.org/10.3390/en13010158.
[36] Ebeed M, Aleem SHEA. Chapter 1 - Overview of uncertainties in modern power systems: uncertainty models and methods. In: Zobaa AF, Abdel Aleem SHEBT-U in MPS, editors., Academic Press; 2021, p. 1–34. doi:https://doi.org/10.1016/B978-0-12-820491-7.00001-3.
[37] Hemeida AM, El-Ahmar MH, El-Sayed AM, Hasanien HM, Alkhalaf S, Esmail MFC, et al. Optimum design of hybrid wind/PV energy system for remote area. Ain Shams Eng J 2020;11:11–23. doi: https://doi.org/10.1016/j.asej.2019.08.005.
[38] Bai W, Eke I, Lee KY. An improved artificial bee colony optimization algorithm based on orthogonal learning for optimal power flow problem. Control Eng Pract 2017;61:163–72. doi: https://doi.org/10.1016/j.conengprac.2017.02.010.
[39] Biswas PP, Suganthan PN, Amaratunga GAJ. Optimal power flow solutions incorporating stochastic wind and solar power. Energy Convers Manag 2017;148:1194–207. doi: https://doi.org/10.1016/j.enconman.2017.06.071.
[40] Mostafa MH, Abdel Aleem SHE, Ali SG, Ali ZM, Abdelaziz AY. Techno-economic assessment of energy storage systems using annualized life cycle cost of storage (LCCOS) and levelized cost of energy (LCOE) metrics. J Energy Storage 2020;29:. doi: https://doi.org/10.1016/j.est.2020.101345101345.
[41] Hulio ZH, Jiang W, Rehman S. Techno - economic assessment of wind power potential of Hawke's Bay using Weibull parameter: A review. Energy Strateg Rev 2019;26:. doi: https://doi.org/10.1016/j.esr.2019.100375100375.
[42] Qais MH, Hasanien HM, Alghuwainem S. Low voltage ride-through capability enhancement of grid-connected permanent magnet synchronous generator driven directly by variable speed wind turbine: a review. J Eng 2017;2017:1750–4. doi: https://doi.org/10.1049/joe.2017.0632.

[43] Hamilton WT, Husted MA, Newman AM, Braun RJ, Wagner MJ. Dispatch optimization of concentrating solar power with utility-scale photovoltaics. Optim Eng 2020;21:335–69. doi: https://doi.org/10.1007/s11081-019-09449-y.
[44] de la Calle A, Bayon A, Pye J. Techno-economic assessment of a high-efficiency, low-cost solar-thermal power system with sodium receiver, phase-change material storage, and supercritical CO2 recompression Brayton cycle. Sol Energy 2020;199:885–900. doi: https://doi.org/10.1016/j.solener.2020.01.004.
[45] Gómez YM, Bolfarine H, Gómez HW. Gumbel distribution with heavy tails and applications to environmental data. Math Comput Simul 2019;157:115–29. doi: https://doi.org/10.1016/j.matcom.2018.10.003.
[46] Eshra NM, Zobaa AF, Abdel Aleem SHE. Assessment of mini and micro hydropower potential in Egypt: Multi-criteria analysis. Energy Rep 2021;7:81–94. doi: https://doi.org/10.1016/j.egyr.2020.11.165.
[47] Diaaeldin I, Aleem SA, El-Rafei A, Abdelaziz A, Zobaa AF. Optimal network reconfiguration in active distribution networks with soft open points and distributed generation. Energies 2019;12:4172. doi: https://doi.org/10.3390/en12214172.
[48] Mirjalili S, Mirjalili SM, Lewis A. Grey wolf optimizer. Adv Eng Softw 2014;69:46–61. doi: https://doi.org/10.1016/j.advengsoft.2013.12.007.
[49] Kamboj VK, Bath SK, Dhillon JS. Solution of non-convex economic load dispatch problem using grey wolf optimizer. Neural Comput Appl 2016;27:1301–16. doi: https://doi.org/10.1007/s00521-015-1934-8.
[50] Jayakumar N, Subramanian S, Ganesan S, Elanchezhian EB. Grey wolf optimization for combined heat and power dispatch with cogeneration systems. Int J Electr Power Energy Syst 2016;74:252–64. doi: https://doi.org/10.1016/j.ijepes.2015.07.031.
[51] Omar A, HE Abdel Aleem S, EA El-Zahab E, Bendary F. A Robust D-FACTS Based Metaheuristic Control System for Battery Charging Scheme 2019.
[52] Sahoo BP, Panda S. Improved grey wolf optimization technique for fuzzy aided PID controller design for power system frequency control. Sustain Energy, Grids Networks 2018;16:278–99. doi: https://doi.org/10.1016/j.segan.2018.09.006.
[53] Qais MH, Hasanien HM, Alghuwainem S. A grey wolf optimizer for optimum parameters of multiple PI controllers of a grid-connected PMSG driven by variable speed wind turbine. IEEE Access 2018;6:44120–8. doi: https://doi.org/10.1109/ACCESS.2018.2864303.
[54] Qais MH, Hasanien HM, Alghuwainem S. Augmented grey wolf optimizer for grid-connected PMSG-based wind energy conversion systems. Appl Soft Comput 2018;69:504–15. doi: https://doi.org/10.1016/j.asoc.2018.05.006.
[55] Kumar A, Sah B, Singh AR, Deng Y, He X, Kumar P, et al. A review of multi criteria decision making (MCDM) towards sustainable renewable energy development. Renew Sustain Energy Rev 2017;69:596–609. doi: https://doi.org/10.1016/j.rser.2016.11.191.
[56] Ilbahar E, Cebi S, Kahraman C. A state-of-the-art review on multi-attribute renewable energy decision making. Energy Strateg Rev 2019;25:18–33. doi: https://doi.org/10.1016/j.esr.2019.04.014.
[57] Saaty RW. The analytic hierarchy process-what it is and how it is used. Math Model 1987;9:161–76. doi: https://doi.org/10.1016/0270-0255(87)90473-8.
[58] Moutinho L, Hutcheson G, Beynon MJ. Analytic Hierarchy Process. SAGE Dict. Quant. Manag. Res., 1 Oliver's Yard, 55 City Road, London EC1Y 1SP United Kingdom: SAGE Publications Ltd; 2014, p. 9–12. doi:10.4135/9781446251119.n3.
[59] Wang J, Chakraborty C, Ouyang H. The analytic hierarchy process. Encycl. Decis. Mak. Decis. Support Technol. 2011. doi: https://doi.org/10.4018/978-1-59904-843-7.ch003.
[60] Saaty TL. Decision making with the analytic hierarchy process. Int J Serv Sci 2008;1:83. doi: https://doi.org/10.1504/IJSSCI.2008.017590.
[61] Wang CN, Nguyen VT, Thai HTN, Duong DH. Multi-criteria decision making (MCDM) approaches for solar power plant location selection in Viet Nam. Energies 2018;11:1504. doi: https://doi.org/10.3390/en11061504.
[62] Dehghanian P, Fotuhi-Firuzabad M, Bagheri-Shouraki S, Razi Kazemi AA. Critical component identification in reliability centered asset management of power distribution systems via fuzzy AHP. IEEE Syst J 2012;6:593–602. doi: https://doi.org/10.1109/JSYST.2011.2177134.
[63] Abdel Aleem SHE, Zobaa AF, Abdel Mageed HM. Assessment of energy credits for the enhancement of the Egyptian green pyramid rating system. Energy Policy 2015;87:407–16. doi: https://doi.org/10.1016/j.enpol.2015.09.033.
[64] Elbasuony GS, Abdel Aleem SHE, Ibrahim AM, Sharaf AM. A unified index for power quality evaluation in distributed generation systems. Energy 2018;149:607–22. doi: https://doi.org/10.1016/j.energy.2018.02.088.
[65] Ho W, Ma X. The state-of-the-art integrations and applications of the analytic hierarchy process. Eur J Oper Res 2018;267:399–414. doi: https://doi.org/10.1016/j.ejor.2017.09.007.
[66] Bahmanifirouzi B, Farjah E, Niknam T, Azad Farsani E. A new hybrid hbmo-sfla algorithm for multi-objective distribution feeder reconfiguration problem considering distributed generator units. Iran J Sci Technol - Trans Electr Eng 2012;36:51–66.
[67] Chen G, Yi X, Zhang Z, Lei H. Solving the multi-objective optimal power flow problem using the multi-objective firefly algorithm with a constraints-prior pareto-domination approach. Energies 2018;11. doi: https://doi.org/10.3390/en11123438.
[68] Abdullah M, Javaid N, Chand A, Khan ZA, Waqas M, Abbas Z. Multi-objective optimal power flow using improved multi-objective multi-verse algorithm. In: Barolli L, Takizawa M, Xhafa F, Enokido T, editors. Adv. Intell. Syst. Comput., vol. 927, Cham: Springer International Publishing; 2019, p. 1071–83. doi:10.1007/978-3-030-15035-8_104.

Muhyaddin Rawa received a BSc degree in Electrical and Computer Engineering from Umm Al-Qura University, an MSc degree in Electrical and Computer Engineering, Power and Machines, from King Abdulaziz University and a PhD in electrical and electronic engineering from the University of Nottingham in 2000, 2008 and 2014, respectively. He has more than 7 years experience in Saudi Electricity Company before joining the Department of Electrical and Computer Engineering at King Abdulaziz University in 2008. Dr. Muhyaddin is the deputy director of Center of Research Excellence in Renewable Energy and Power Systems. He is actively involved in industrial consultancy for major corporations in power systems projects. His research interest includes power quality, renewable energy and smart grids. Dr Muhyaddin is a member of IEEE.

Abdullah Abusorrah (M'08-SM'14) is a Professor in the Department of Electrical and Computer Engineering at King Abdulaziz University. He is the head of the Center for Renewable Energy and Power Systems at King Abdulaziz University. His field of interest includes renewable energy, smart grid and system analysis. He received his PhD degree in Electrical Engineering from the University of Nottingham in United Kingdom in 2007.

Dr H. Bassi (M'08) received his Bc.S degree in Electrical and Computer Engineering from King Abdulaziz University in 2003 and M.S Degree in Electrical Engieering from Florida Institute of Technolgy. In 2008 he received a PhD degree in Electrical Engieering from University of Pittsburgh in 2013. He is currently an assistant professor at King Abdulaziz Universtiy to teach major courses in the department of electrical engineering ranges from the low-level courses to more advanced ones such as power system transients and Photovoltaic Systems. He contributes effectively to his discipline by adding innovative ideas and compete to add upon the state-of-the-art in power electronics technologies and renewable energy.Dr. Bassi woked as a site superintendent to monitor day-to-day construction activities at the working sites, even under high-pressure conditions, while maintaining the required loss prevention regulations. He was continuously updating his technical and managerial knowledge to handle the projects professionally. He worked for project management team (PMT) department at SAUDI ARAMCO to complete projects in instrumentation and power engineering areas until 2005.

Saad Mekhilef (Senior Member, IEEE) received the B. Eng. degree in electrical engineering from the University of Setif, Setif, Algeria, in 1995, and the master's degree in engineering science and the Ph.D. degree in electrical engineering from the University of Malaya, Kuala Lumpur, Malaysia, in 1998 and 2003, respectively. He is currently a Professor and the Director of the Power Electronics and Renewable Energy Research Laboratory, Department of Electrical Engineering, University of Malaya. He is also the Dean of the Faculty of Engineering, University of Malaya. He is also a Distinguished Adjunct Professor with the Faculty of Science, Engineering and Technology, School of Software and Electrical Engineering, Swinburne University of Technology, VIC, Australia. He has authored or coauthored more than 400 publications in international journals and conference proceedings. His current research interests include power converter topologies, control of power converters, renewable energy, and energy efficiency.

Ziad M. Ali received a B.Sc. degree in electrical engineering from Assiut University, faculty of engineering, Assuit, Egypt, in 1998. He worked as a demonstrator in Aswan faculty of engineering, south valley university, Aswan, Egypt. He obtained an M.Sc. degree from Assiut University, faculty of engineering in electrical engineering in 2003. He worked as Assistant Lecturer in Aswan faculty of Engineering. He got a Ph.D. degree in 2010 from Kazan State Technical University, Tatarstan, Russia. He is the author or co-author of many refereed journals and conference papers. He is currently working as Associate Professor in Electrical Dept. College of Engineering at Wadi Addawasir, Prince Sattam bin Abdulaziz University, Saudi Arabia.

Shady H. E. Abdel Aleem (M'12, SM'21) received B.Sc., M.Sc. and Ph.D. degrees in Electrical Power and Machines from the Faculty of Engineering, Helwan University, Egypt, in 2002, and the Faculty of Engineering, Cairo University, Egypt, in 2010 and 2013, respectively. He is currently an Associate Professor at the College of Engineering and Technology, Arab Academy for Science, Technology and Maritime Transport, Energy Department, Smart Village, Egypt, and head of the consultancy office in ETA Electric Company, Egypt. His research interests include power systems, power quality, renewable energy, smart grid, electric machines, and optimization. He was awarded the State Encouragement Award in Engineering Sciences in 2017 from Egypt and a medal of scientific excellence in Engineering Sciences in 2020 from Egypt. He has authored or co-authored more than 130 publications in international journals and conference proceedings. He is an Editorial Board member, an Editor, an Associate Editor, and an Editorial Advisory Board member for many international journals.

Hany M. Hasanien (M 09, SM 11) received his B.Sc., M. Sc. and Ph.D. degrees in Electrical Engineering from Ain Shams University, Faculty of Engineering, Cairo, Egypt, in 1999, 2004, and 2007, respectively. From 2008 to 2011, he was a Joint Researcher with Kitami Institute of Technology, Kitami, Japan. From 2012 to 2015, he was Associate Professor at College of Engineering, King Saud University, Riyadh, Saudi Arabia. Currently, he is Professor at the Electrical Power and Machines Department, Faculty of Engineering, Ain Shams University. His research interests include modern control techniques, power systems dynamics and control, energy storage systems, renewable energy systems, and smart grid. Prof. Hasanien is an Editorial Board Member of *Electric Power Components and Systems Journal*. He is Subject Editor of IET Renewable Power Generation, Ain Shams Engineering Journal and Electronics MDPI. He has authored, co-authored, and edited three books in the field of electric machines and renewable energy. He has published more than 150 papers in international journals and conferences. His biography has been included in *Marquis Who's Who in the world* for its 28 edition, 2011. He was awarded Encouraging Egypt Award for Engineering Sciences in 2012. He was awarded Institutions Egypt Award for Invention and Innovation of Renewable Energy Systems Development in 2014. He was awarded the Superiority Egypt Award for Engineering Sciences in 2019. Currently, he is IEEE PES Egypt Chapter Chair.

Ahmed I. Omar received a B.Sc. degree in Electrical Power and Machines Engineering from The Higher Institute of Engineering at El-Shorouk City in 2011, M. Sc., and Ph.D. degrees in Electrical Power and Machines from the Faculty of Engineering, Cairo University, Egypt, in 2014 and 2019, respectively. Between September 2011 and September 2019, he was a Teaching Assistant at The Higher Institute of Engineering at El-Shorouk City. His research interests include FACTS in power systems, power quality, renewable energy, smart grid, energy efficiency, optimization, green energy, and economics. He is author or co-author of many refereed journals and conference papers. He is a reviewer in many international journals.